

The Optimal Power Flow Operator: Theory and Computation

Fengyu Zhou, James Anderson, and Steven H. Low *

March 26, 2022

Abstract

Optimal power flow problems (OPFs) are mathematical programs used to distribute power over networks subject to network operation constraints and the physics of power flows. In this work we take the view of treating an OPF problem as an operator which maps user demand to generated power and allow the network parameters to take values in some admissible set. The contributions of this paper are to formalize this operator theoretic approach, define and characterize a restricted parameter sets under which the mapping has a singleton output, independent binding constraints, and is differentiable. We further provide a closed-form expression for the Jacobian matrix of the OPF operator and describe how various derivatives can be computed using a recently proposed scheme based on homogenous self-dual embedding. Our framework of treating a mathematical program as an operator allows us to pose sensitivity and robustness questions from a completely different mathematical perspective and provide new insights into well studied problems.

1 Introduction

Given a power network, the optimal power flow (OPF) problem seeks to find an optimal operating point that minimizes an appropriate cost function subject to power flow constraints (e.g. Kirchhoff's laws) and pre-specified network tolerances (e.g. capacity constraints)[8, 19, 10, 14, 13]. The decision variables in an OPF problem are typically voltages and generation power. Cost function choices include minimizing power loss, generation cost, and user disutility.

In this work we consider the direct current (DC) model of the power flow equations [32, 33, 35]. The DC OPF problem is widely used in industry and takes the form of a linear

*J. Anderson and S. Low are with the Department of Computing + Mathematical Sciences, F. Zhou is with the Department of Electrical Engineering, both at the California Institute of Technology, Pasadena CA, 91125.

program (LP) [6, 9]. Consider a power network with N_G generators and N_L loads, the problem is formulated as

$$\underset{\mathbf{s}^g}{\text{minimize}} \quad \mathbf{f}^\top \mathbf{s}^g \quad (1a)$$

$$\text{subject to} \quad \mathbf{A}_{\text{eq}} \mathbf{s}^g = \mathbf{b}_{\text{eq}}(\mathbf{s}^l, \mathbf{b}') \quad (1b)$$

$$\mathbf{A}_{\text{in}} \mathbf{s}^g \leq \mathbf{b}_{\text{in}} \quad (1c)$$

where $\mathbf{s}^g \in \mathbb{R}^{N_G}$ is the decision vector of power generations at each generator node in the network. The equality constraint function \mathbf{b}_{eq} is linear in \mathbf{s}^l (the vector of power demands at each node) and \mathbf{b}' . We view \mathbf{f} , \mathbf{b}' and \mathbf{b}_{in} as system parameters, whose values are allowed to change in a set Ω . Matrices \mathbf{A}_{eq} and \mathbf{A}_{in} are determined by network topology and susceptances. We treat the power demand \mathbf{s}^l , which is allowed to take values in the set $\Omega_{\mathbf{s}^l}$, as an “input” and the optimal generations $(\mathbf{s}^g)^*$ as an “output”. One of the main contributions of this work is to study the DC OPF problem (1) as an operator, in particular we define

$$\mathcal{OPF} : \Omega_{\mathbf{s}^l} \rightarrow 2^{\mathcal{S}}$$

where $\mathcal{S} \subset \mathbb{R}^{N_G}$ and $2^{\mathcal{S}}$ denotes the power set of \mathcal{S} . We study the following questions in this paper:

- When is \mathcal{OPF} a singleton in \mathcal{S} ?
- What restrictions are required on the sets Ω and $\Omega_{\mathbf{s}^l}$ for (1) to have independent binding constraints?
- Do the above restrictions form dense subsets of Ω and $\Omega_{\mathbf{s}^l}$?
- Under what conditions is \mathcal{OPF} differentiable with respect to changes in \mathbf{s}^l (when the output of \mathcal{OPF} is a singleton in the neighborhood of \mathbf{s}^l)?
- What is the structure of the Jacobian matrix of \mathcal{OPF} ?

We show that certain subsets of Ω and $\Omega_{\mathbf{s}^l}$ endow the \mathcal{OPF} with uniqueness of solution and appropriate smoothness properties. Furthermore, these subsets are dense and thus, when a specific problem instance falls outside of the sets, a slightly perturbed version will be in these subsets. With regards to the Jacobian matrix, we provide two perspectives. The first is in terms of the problem data describing (1) and the second is described purely in terms of a discrete, graphical representation of the problem. We prove that the two perspectives are equivalent in the sense that for any Jacobian matrix constructed from one formulation, we can find the variables from the other and reconstruct the same matrix. Although not the main focus of this paper we describe how various derivatives can be computed using some recently developed ideas from [1, 2] that uses a homogenous self-dual embedding technique [36].

Whilst the above issues may seem technical, they are in fact the building blocks for many applications. Establishing uniqueness of solution is a fundamental property of an operator as it provides the foundation for defining a derivative. Moreover, many numerical

techniques require unique solutions to ensure convergence. Characterizing the set of independent binding constraints paves the road for many further theoretical analyses. In [30], it is shown that even under significant load variations, the number of binding line constraints in the DC-OPF problem is frequently a small proportion of the total number of constraints - an observation which has significant implications when it comes to long-term planning and assessing network vulnerability [21]. In [15], the set of binding constraints determines an area of load profiles (termed System Pattern Regions by the authors) within which the vector of locational marginal prices remain constant. Establishing the set of independent binding constraints also allows us to produce a closed form expression for the Jacobian matrix, which can serve as the main tool to study the system sensitivity. In recent works we showed that “worst-case” sensitivity bounds provide privacy guarantees when releasing power flow data [39] and for data disaggregation [3]. In the context of real-time optimization where sensitivity is often assumed to be known and bounded [34], this work can be used to provide exactly these bounds (or rule them out).

1.1 Related Work

Our approach to sensitivity analysis differs from the standard perturbation approach which assumes the constraints are shifted from their nominal right-hand sides, and then looks at the Lagrange multipliers, see for example [7, Ch. 5.6]. In this setting one considers the optimization problem

$$\begin{aligned} & \underset{\mathbf{x}}{\text{minimize}} && \mathbf{f}_0(\mathbf{x}) \\ & \text{subject to} && \mathbf{f}_i(\mathbf{x}) \leq \mathbf{u}_i, \quad i = 1, \dots, m, \\ & && \mathbf{h}_j(\mathbf{x}) = \mathbf{v}_j, \quad j = 1, \dots, p, \end{aligned} \tag{2}$$

where $\mathbf{x} \in \mathbb{R}^n$ is the decision vector. Let us assume that strong duality holds for (2). The *nominal* problem consists of setting \mathbf{u}_i and \mathbf{v}_j to zero for all i and j . The nominal optimal value is denoted by \mathbf{x}^* . The *perturbed* problem is obtained by adjusting the right-hand side of the equalities and inequalities, thus tightening or relaxing these constraints. The perturbed optimal value is denoted by $p^*(\mathbf{u}, \mathbf{v})$. Let $\boldsymbol{\lambda}^*$ and $\boldsymbol{\nu}^*$ denote the vectors of optimal Lagrange multipliers for the nominal problem. Then we have the following well known lower-bound for the perturbed problem $p^*(\mathbf{u}, \mathbf{v}) \geq p^*(\mathbf{0}, \mathbf{0}) - \boldsymbol{\lambda}^{*\top} \mathbf{u} - \boldsymbol{\nu}^{*\top} \mathbf{v}$. Additionally, the magnitude (and sign in the case of $\boldsymbol{\nu}^*$) provide information regarding the sensitivity of $p^*(\mathbf{u}, \mathbf{v})$ with respect to constraints being tightened and relaxed. Furthermore, under differentiability assumptions on $p^*(\mathbf{u}, \mathbf{v})$ (and again under the strong duality assumption), the optimal Lagrange multipliers characterize the local sensitivities of the optimal value with respect to constraint perturbations. Concretely, the sensitivities are given by the relations $\lambda_i^* = -\partial_{\mathbf{u}_i} p^*(\mathbf{0}, \mathbf{0})$ and $\nu_j^* = -\partial_{\mathbf{v}_j} p^*(\mathbf{0}, \mathbf{0})$. This approach differs from our problem in the following ways. First, we focus on the perturbation of the optimal solution, rather than the optimal value. Second, we focus more on the set of binding constraints and whether they are independent, as opposed to appealing to duality.

Perhaps the most obvious body of work to compare to is that of robust optimization [4, 5, 28] and stochastic optimization [18, 20, 25]. Consider the linear program $\{\text{minimize}_{\mathbf{x}} \mathbf{c}^\top \mathbf{x} : \mathbf{A}\mathbf{x} \leq \mathbf{b}, (\mathbf{A}, \mathbf{b}, \mathbf{c}) \in \mathcal{U}\}$. In the robust optimization setting, the set \mathcal{U} encodes deterministic uncertainty in the problem data. The objective is thus to minimize the decision vector x over all allowable instantiations of the uncertainty. In the stochastic setting, the same philosophy is applied. The set \mathcal{U} encodes distributions from which the problem data is drawn and the cost function is then suitably defined. In both cases, the goal is to mitigate the effects of uncertainty. In contrast, our work seeks to determine how the optimal decision changes with respect to data perturbations. Our results can thus be considered complementary to the robust and stochastic optimization frameworks.

There has been some work which specifically defines and studies the DC OPF sensitivity [16, 37, 26]. In [16, 37], the OPF problem is formulated as a parameterized optimization problem [17] where the loads, the upper and lower bounds for generations and branch power flows are all parameterized by ϵ . At the point $\epsilon = 0$, the sensitivity, defined as the derivative of the optimal solution with respect to ϵ , can be computed from the KKT conditions, assuming it is known which constraints are binding and the values of the optimal solution and Lagrangian multipliers are available at $\epsilon = 0$. In the work mentioned above, there is only a single degree of freedom in parameter variation, and differentiability is checked by going through an involved procedure for each OPF problem. On the contrary, we generalize the concept of sensitivity to the Jacobian matrix, which allows the parameters to change in various directions. Instead of checking differentiability for each problem, we explicitly characterize the sets of parameters that guarantee differentiability, and based on the fact that those sets are all dense within the spaces of interest, we conclude that differentiability can always be assumed up to parameter perturbation. Furthermore, we provide numerical methods to compute the derivatives.

1.2 Article Outline

The remainder of this paper is organized as follows. In Section 2, we formalize the DC OPF problem, and characterize the parameter set of interest under which the OPF problem is feasible and has optimal solutions. For the parameters in the set of interest, we define the associated operator that maps the load to the set of optimal generations. In Section 3, we restrict the set of interest to those parameters that endow the OPF operator with the following properties: the operator always maps to a singleton and the binding constraints are independent. We also show that the restricted set is dense within the set of interest, so the restriction does not lose generality up to perturbation. In Section 4, we prove the operator is differentiable for parameters in the restricted set and derive the closed form expression of the Jacobian matrix in terms of the independent binding constraints. Moreover, we prove there exist a surjection between the restricted set and the set of independent binding constraints such that the derivative of the operator and the Jacobian matrix in terms of binding constraints take the same value under such surjection. While the former characterizes how sensitive the OPF operator is, the latter only depends on the graph topology and has a closed form expression. In Section 5, we also demonstrate that an algorithm introduced in

recent work [1, 2] can help numerically evaluate the operator differentiation and extend the results to the alternating current (AC) OPF case. Finally, Section 6 provides a numerical example and graphically illustrates the parameter sets of interest and restricted sets for a simple test network.

2 Background

In this section we define the power network model and the optimal power flow problem.

Notation

Vectors and matrices are typically written in bold while scalars are not. Given two vectors $\mathbf{a}, \mathbf{b} \in \mathbb{R}^n$, $\mathbf{a} \geq \mathbf{b}$ denotes the element-wise partial order $\mathbf{a}_i \geq \mathbf{b}_i$ for $i = 1, \dots, n$. For a scalar k , we define the projection operator $[k]^- := \min\{0, k\}$. We define $\|\mathbf{x}\|_0$ as the number of non-zero elements of the vector \mathbf{x} . Identity and zero matrices are denoted by \mathbf{I}^n and $\mathbf{0}^{n \times m}$ while vectors of all ones are denoted by $\mathbf{1}_n$ where superscripts and subscripts indicate their dimensions. To streamline notation, we omit the dimensions when the context makes it clear. The notation \mathbb{R}_+ denotes the non-negative real set $[0, +\infty)$. For $\mathbf{X} \in \mathbb{R}^{n \times m}$, the restriction $\mathbf{X}_{\{1,3,5\}}$ denotes the $3 \times m$ matrix composed of stacking rows 1, 3, and 5 on top of each other. We will frequently use a set to describe the rows we wish to form the restriction from, in this case we assume the elements of the set are arranged in increasing order. We will use \mathbf{e}_m to denote the standard base for the m^{th} coordinate, its dimension will be clear from the context. Let $(\cdot)^\dagger$ be the Moore-Penrose inverse. Denote $[m] := \{1, 2, \dots, m\}$ and $[n, m] := \{n, n+1, \dots, m\}$. Finally, for a convex set $\mathcal{X} \subseteq \mathbb{R}^n$ and vector $\mathbf{x} \in \mathbb{R}^n$, we let $\mathcal{P}_{\mathcal{X}}\mathbf{x}$ be the projection of \mathbf{x} onto the set \mathcal{X} . By isometry, the domain of the projection operator is extended to matrices when needed.

2.1 System Model

Consider a power network modeled by an undirected connected graph $\mathcal{G}(\mathcal{V}, \mathcal{E})$, where $\mathcal{V} := \mathcal{V}_G \cup \mathcal{V}_L$ denotes the set of buses which can be further classified into generators in set \mathcal{V}_G and loads in set \mathcal{V}_L , and $\mathcal{E} \subseteq \mathcal{V} \times \mathcal{V}$ is the set of all branches linking those buses. We will later use the terms (graph, vertex, edge) and (power network, bus, branch) interchangeably. Suppose $\mathcal{V}_G \cap \mathcal{V}_L = \emptyset$ and there are $|\mathcal{V}_G| =: N_G$ generator and $|\mathcal{V}_L| =: N_L$ loads, respectively. For simplicity, let $\mathcal{V}_G = [N_G]$, $\mathcal{V}_L = [N_G + 1, N_G + N_L]$. Let $N = N_G + N_L$. Without loss of generality, \mathcal{G} is a connected graph with $|\mathcal{E}| =: E$ edges labelled as $1, 2, \dots, E$. Let $\mathbf{C} \in \mathbb{R}^{N \times E}$ be the signed incidence matrix. We will use e , (u, v) or (v, u) interchangeably to denote the same edge. Let $\mathbf{B} = \text{diag}(b_1, b_2, \dots, b_E)$, where $b_e > 0$ is the susceptance of branch e . As we adopt a DC power flow model, all branches are assumed lossless. Further, we denote the generation and load as $\mathbf{s}^g \in \mathbb{R}^{N_G}$, $\mathbf{s}^l \in \mathbb{R}^{N_L}$, respectively. Thus \mathbf{s}_i^g refers to the generation on bus i while \mathbf{s}_i^l refers to the load on bus $N_G + i$. We will refer to bus $N_G + i$ simply as load i for simplicity. The power flow on branch $e \in \mathcal{E}$ is denoted as \mathbf{p}_e , and $\mathbf{p} := [\mathbf{p}_1, \dots, \mathbf{p}_E]^\top \in \mathbb{R}^E$.

is the vector of all branch power flows. To simplify analysis, we assume that there are no buses in the network that are both loads and generators. This is stated formally below:

Assumption 1. $\mathcal{V}_G \cap \mathcal{V}_L = \emptyset$.

The above assumption is not restrictive. We can always split a bus with both a generator and a load into a bus with only the generator adjacent to another bus with only the load, and connect all the neighbors of the original bus to that load bus.

2.2 DC Optimal Power Flow

We focus on the DC-OPF problem with a linear cost function [32, 33, 35]. That is to say, the voltage magnitudes are assumed to be fixed and known and the lines are considered to be lossless. Without loss of generality, we assume all the voltage magnitudes to be 1. The decision variables are the voltage angles denoted by vector $\boldsymbol{\theta} \in \mathbb{R}^N$ and power generations \mathbf{s}^g , given loads \mathbf{s}^l . The DC-OPF problem takes the form:

$$\underset{\mathbf{s}^g, \boldsymbol{\theta}}{\text{minimize}} \quad \mathbf{f}^\top \mathbf{s}^g \quad (3a)$$

$$\text{subject to} \quad \boldsymbol{\theta}_1 = 0 \quad (3b)$$

$$\mathbf{CBC}^\top \boldsymbol{\theta} = \begin{bmatrix} \mathbf{s}^g \\ -\mathbf{s}^l \end{bmatrix} \quad (3c)$$

$$\underline{\mathbf{s}}^g \leq \mathbf{s}^g \leq \bar{\mathbf{s}}^g \quad (3d)$$

$$\underline{\mathbf{p}} \leq \mathbf{BC}^\top \boldsymbol{\theta} \leq \bar{\mathbf{p}}. \quad (3e)$$

Here, $\mathbf{f} \in \mathbb{R}_+^{N_G}$ is the unit cost for each generator, and bus 1 is selected as the slack bus with fixed voltage angle 0. In (3c), we let the injections for generators be positive while the injections for loads be the negation of \mathbf{s}^l . The upper and lower limits on the generations are set as $\bar{\mathbf{s}}^g$ and $\underline{\mathbf{s}}^g$, respectively, and $\bar{\mathbf{p}}$ and $\underline{\mathbf{p}}$ are the limits on branch power flows. We assume that (3) is well posed, i.e. $\bar{\mathbf{s}}^g > \mathbf{s}^g \geq 0$, $\bar{\mathbf{p}} > \underline{\mathbf{p}}$. Note that the LP (3) is a particular realization of (1). Our results can be extended to the general case, however we present this paper assuming the specific problem form of (3). We stress that no knowledge of power engineering is needed to derive or understand the results in this paper.

Let $\boldsymbol{\tau} \in \mathbb{R}^{N+1}$ be the vector of Lagrangian multipliers associated with equality constraints (3b), (3c), and $(\boldsymbol{\lambda}_+, \boldsymbol{\lambda}_-)$ and $(\boldsymbol{\mu}_+, \boldsymbol{\mu}_-)$ be the Lagrangian multipliers associated with inequalities (3d) and (3e) respectively. As (3) is a linear program [6], the following KKT condition holds at an optimal point when (3) is feasible:

$$(3b) - (3e) \quad (4a)$$

$$\mathbf{0} = \mathbf{M}^\top \boldsymbol{\tau} + \mathbf{CB}(\boldsymbol{\mu}_+ - \boldsymbol{\mu}_-) \quad (4b)$$

$$-\mathbf{f} = -[\boldsymbol{\tau}_1, \boldsymbol{\tau}_2, \dots, \boldsymbol{\tau}_{N_G}]^\top + \boldsymbol{\lambda}_+ - \boldsymbol{\lambda}_- \quad (4c)$$

$$\boldsymbol{\mu}_+, \boldsymbol{\mu}_-, \boldsymbol{\lambda}_+, \boldsymbol{\lambda}_- \geq 0 \quad (4d)$$

$$\boldsymbol{\mu}_+^\top (\mathbf{BC}^\top \boldsymbol{\theta} - \bar{\mathbf{p}}) = \boldsymbol{\mu}_-^\top (\underline{\mathbf{p}} - \mathbf{BC}^\top \boldsymbol{\theta}) = 0 \quad (4e)$$

$$\boldsymbol{\lambda}_+^\top (\mathbf{s}^g - \bar{\mathbf{s}}^g) = \boldsymbol{\lambda}_-^\top (\underline{\mathbf{s}}^g - \mathbf{s}^g) = 0, \quad (4f)$$

where

$$\mathbf{M} := \begin{bmatrix} \mathbf{CBC}^\top \\ \mathbf{e}_1^\top \end{bmatrix}$$

is an $(N + 1)$ -by- N matrix with rank N and \mathbf{e}_1 denotes the standard first basis vector. Condition (4a) corresponds to primal feasibility, condition (4d) corresponds to dual feasibility, conditions (4e), (4f) correspond to complementary slackness, and conditions (4b), (4c) correspond to stationarity [7].

2.3 OPF as an Operator: \mathcal{OPF}

In this section we will describe how we formulate the DC-OPF (3) as a mapping from load to (optimal) generation space. We assume throughout the paper that the topology of the network remains constant, as do the line susceptances. These assumptions imply that the graph Laplacian given by \mathbf{CBC}^\top does not change. Let $\boldsymbol{\xi} := [(\bar{\mathbf{s}}^g)^\top, (\underline{\mathbf{s}}^g)^\top, \bar{\mathbf{p}}^\top, \underline{\mathbf{p}}^\top]^\top \in \mathbb{R}^{2N_G+2E}$ be the vector of system limits. Define

$$\Omega_{\boldsymbol{\xi}} := \{\boldsymbol{\xi} \mid \underline{\mathbf{s}}^g \geq 0, (3b) - (3e) \text{ are feasible for some } \mathbf{s}^l > 0\}.$$

The set $\Omega_{\boldsymbol{\xi}}$ defines the set of power flow and generation limits such that the DC-OPF is primal-dual feasible and makes physical sense i.e. upper-limits are greater than lower-limits. Note that $\Omega_{\boldsymbol{\xi}}$ does not depend on the cost vector \mathbf{f} .

Proposition 2.1. *The set $\Omega_{\boldsymbol{\xi}}$ satisfies $\text{clos}(\text{int}(\Omega_{\boldsymbol{\xi}})) = \text{clos}(\Omega_{\boldsymbol{\xi}})$.*

Proof. See Appendix A. ■

For each $\boldsymbol{\xi} \in \Omega_{\boldsymbol{\xi}}$, define ¹

$$\Omega_{\mathbf{s}^l}(\boldsymbol{\xi}) := \{\mathbf{s}^l \mid \mathbf{s}^l > 0, (3b) - (3e) \text{ are feasible}\}.$$

Then $\Omega_{\mathbf{s}^l}(\boldsymbol{\xi})$ is convex and nonempty. When we fix $\boldsymbol{\xi}$ and there is no confusion, we simply write $\Omega_{\mathbf{s}^l}$.

Definition 1. *Define $\Omega := \{(\mathbf{f}, \boldsymbol{\xi}, \mathbf{s}^l) \mid \mathbf{f} \in \mathbb{R}_+^{N_G}, \boldsymbol{\xi} \in \Omega_{\boldsymbol{\xi}}, \mathbf{s}^l \in \Omega_{\mathbf{s}^l}(\boldsymbol{\xi})\}$.*

When $\boldsymbol{\xi} \in \Omega_{\boldsymbol{\xi}}, \mathbf{s}^l \in \Omega_{\mathbf{s}^l}(\boldsymbol{\xi})$, the problem (3) is feasible. Since the feasible set of (3) is compact, the solutions to (3) always exist. We now define the operator \mathcal{OPF} , which will be used throughout the rest of the paper.

Definition 2. *Fix $\boldsymbol{\xi} \in \Omega_{\boldsymbol{\xi}}$ and $\mathbf{s}^l \in \Omega_{\mathbf{s}^l}(\boldsymbol{\xi})$, let the set valued operator $\mathcal{OPF} : \Omega_{\mathbf{s}^l} \rightarrow 2^{\mathbb{R}^{N_G}}$ be the mapping such that $\mathcal{OPF}(\mathbf{x})$ is the set of optimal solutions to (3) with parameter $\mathbf{s}^l = \mathbf{x}$.*

In the following section we will establish various properties of the \mathcal{OPF} operator and show that it is a valuable tool for gaining insight into the sensitivity, robustness, and structure of the DC OPF problem (3).

¹In practice, if a load has 0 value, one could replace it by an arbitrarily small positive value so that the load profile is always strictly positive.

3 Operator Properties

We assume that the network topology \mathbf{C} and susceptance \mathbf{B} are always fixed. The operator \mathcal{OPF} is affected by the parameters \mathbf{f} , $\boldsymbol{\xi}$ and \mathbf{s}^l . The set Ω defined in Definition 1 prescribes all the parameters under which (3) is feasible. In this section, we restrict the parameter set so as to endow the operator \mathcal{OPF} with desirable properties.

3.1 Uniqueness

We are specifically interested in the case when the OPF operator defined above maps to a singleton. Let $\Omega_{\mathbf{f}}$ be the set of vectors $\mathbf{f} \geq 0$ such that $\forall \boldsymbol{\xi} \in \Omega_{\boldsymbol{\xi}}, \forall \mathbf{s}^l \in \Omega_{\mathbf{s}^l}(\boldsymbol{\xi})$,

- (3) has a unique solution;
- all solutions to (4) satisfy

$$\|\boldsymbol{\mu}_+\|_0 + \|\boldsymbol{\mu}_-\|_0 + \|\boldsymbol{\lambda}_+\|_0 + \|\boldsymbol{\lambda}_-\|_0 \geq N_G - 1. \quad (5)$$

Proposition 3.1. $\Omega_{\mathbf{f}}$ is dense in $\mathbb{R}_+^{N_G}$.

Proof. See Appendix B. ■

Proposition 3.1 shows that for a fixed network, it is easy to find an objective vector \mathbf{f} such that (3) will always have a unique solution for feasible \mathbf{s}^l . For the remainder of the paper, the following assumption is in play:

Assumption 2. *The objective vector \mathbf{f} is in $\Omega_{\mathbf{f}}$.*

This assumption ensures that (3) has to have a unique solution. When Assumption 2 does not hold, Proposition 3.1 implies that we can always perturb \mathbf{f} such that the assumption is valid.

Remark 3.2. *Under Assumption 2, the value of \mathcal{OPF} is always a singleton, so we can overload $\mathcal{OPF}(\mathbf{x})$ as the function mapping from \mathbf{x} to the unique optimal solution of (3) with parameter $\mathbf{s}^l = \mathbf{x}$.² Since the solution set to the parametric linear program is both upper and lower hemi-continuous [38], \mathcal{OPF} is continuous as well.*

3.2 Independent Binding Constraints

The analysis on the OPF operator can usually be simplified if the set of binding (active) constraints at the optimal point is independent. Here, binding constraints refer to the set of equality constraints (3b), (3c) and those inequality constraints (3d), (3e) for which either

²Except for Appendix D where \mathcal{OPF} is still viewed as a set valued function, \mathcal{OPF} will be viewed as a vector valued function throughout the paper by default.

the upper or lower-bounds are active. Grouping the coefficients of these constraints into a single matrix \mathbf{Z} we refer to them as being independent if \mathbf{Z} is full-rank. Finally, define

$$\begin{aligned} \tilde{\Omega}_{\mathbf{s}^l}(\boldsymbol{\xi}, \mathbf{f}) &:= \{\mathbf{s}^l \in \Omega_{\mathbf{s}^l}(\boldsymbol{\xi}) \mid (3) \text{ has exactly } N_G - 1 \text{ binding inequalities} \\ &\quad \text{at the optimal point, given } \mathbf{s}^l\}. \end{aligned}$$

When \mathbf{f} is fixed, we shorten $\tilde{\Omega}_{\mathbf{s}^l}(\boldsymbol{\xi}, \mathbf{f})$ as $\tilde{\Omega}_{\mathbf{s}^l}(\boldsymbol{\xi})$. Further, if $\boldsymbol{\xi}$ is also fixed, then we will simply use $\tilde{\Omega}_{\mathbf{s}^l}$.

Then we have the following proposition.

Proposition 3.3. *For a fixed $\mathbf{f} \in \Omega_{\mathbf{f}}$, there exists a dense set $\tilde{\Omega}_{\boldsymbol{\xi}}(\mathbf{f}) \subseteq \Omega_{\boldsymbol{\xi}}$ such that $\forall \boldsymbol{\xi} \in \tilde{\Omega}_{\boldsymbol{\xi}}(\mathbf{f})$, the following statements are true:*

- $\text{clos}(\text{int}(\Omega_{\mathbf{s}^l}(\boldsymbol{\xi}))) = \text{clos}(\Omega_{\mathbf{s}^l}(\boldsymbol{\xi}))$.
- $\tilde{\Omega}_{\mathbf{s}^l}(\boldsymbol{\xi}, \mathbf{f})$ is dense in $\Omega_{\mathbf{s}^l}(\boldsymbol{\xi})$.

Proof. See Appendix C. ■

Assumption 3. *The parameter $\boldsymbol{\xi}$ for the limits of generations and branch power flows is assumed to be in $\tilde{\Omega}_{\boldsymbol{\xi}}(\mathbf{f})$, as proposed in Proposition 3.3.*

Assumption 3 allows one to work with set $\tilde{\Omega}_{\boldsymbol{\xi}}(\mathbf{f})$ that are well behaved (where “well behaved” is interpreted as there being exactly $N_G - 1$ binding constraints at the optimal point in the associated DC-OPF problem for almost every \mathbf{s}^l). This assumption is important as in Section 4 it will be needed to show that the derivative of \mathcal{OPF} exists almost everywhere. Moreover, if Assumption 3 does not hold, Proposition 3.3 implies that we can always perturb $\boldsymbol{\xi}$ such that the assumption holds. The proof of Proposition 3.3 can directly extend to the following two corollaries.

Corollary 3.4. *In Proposition 3.3, $\Omega_{\mathbf{s}^l} \setminus \tilde{\Omega}_{\mathbf{s}^l}$ can be covered by the union of finitely many affine hyperplanes.*

Corollary 3.5. *For any $\mathbf{s}^l \in \tilde{\Omega}_{\mathbf{s}^l}$, the $N_G - 1$ tight inequalities in (3), along with $N + 1$ equality constraints, are independent.*

Definition 3. *Define $\tilde{\Omega} := \{(\mathbf{f}, \boldsymbol{\xi}, \mathbf{s}^l) \mid \mathbf{f} \in \Omega_{\mathbf{f}}, \boldsymbol{\xi} \in \tilde{\Omega}_{\boldsymbol{\xi}}(\mathbf{f}), \mathbf{s}^l \in \tilde{\Omega}_{\mathbf{s}^l}(\boldsymbol{\xi}, \mathbf{f})\}$.*

We end this section by summarizing the relationship among the sets $\Omega_{\mathbf{f}}$, $\Omega_{\mathbf{s}^l}$, $\tilde{\Omega}_{\mathbf{s}^l}$, $\Omega_{\boldsymbol{\xi}}$, $\tilde{\Omega}_{\boldsymbol{\xi}}$ defined above using Figure 1. Recall that informally, the set $\Omega_{\boldsymbol{\xi}}$ contains all the $\boldsymbol{\xi}$ that make the OPF problem feasible, and $\Omega_{\mathbf{f}}$ contains \mathbf{f} that guarantee the unique optimal solution for feasible OPF problems and sufficiently many non-zero Lagrange multipliers. Proposition 3.1 shows $\Omega_{\mathbf{f}}$ is dense in $\mathbb{R}_+^{N_G}$. Each $\boldsymbol{\xi} \in \Omega_{\boldsymbol{\xi}}$ maps to a set $\Omega_{\mathbf{s}^l}(\boldsymbol{\xi})$, while each $(\boldsymbol{\xi}, \mathbf{f})$ maps to set $\tilde{\Omega}_{\mathbf{s}^l}(\boldsymbol{\xi}, \mathbf{f})$, which is a subset of $\Omega_{\mathbf{s}^l}(\boldsymbol{\xi})$. For fixed \mathbf{f} , by collecting all the $\boldsymbol{\xi}$ such that $\Omega_{\mathbf{s}^l}(\boldsymbol{\xi})$ has “good” topological property and $\tilde{\Omega}_{\mathbf{s}^l}(\boldsymbol{\xi}, \mathbf{f})$ is dense in $\Omega_{\mathbf{s}^l}(\boldsymbol{\xi})$, we obtain a set

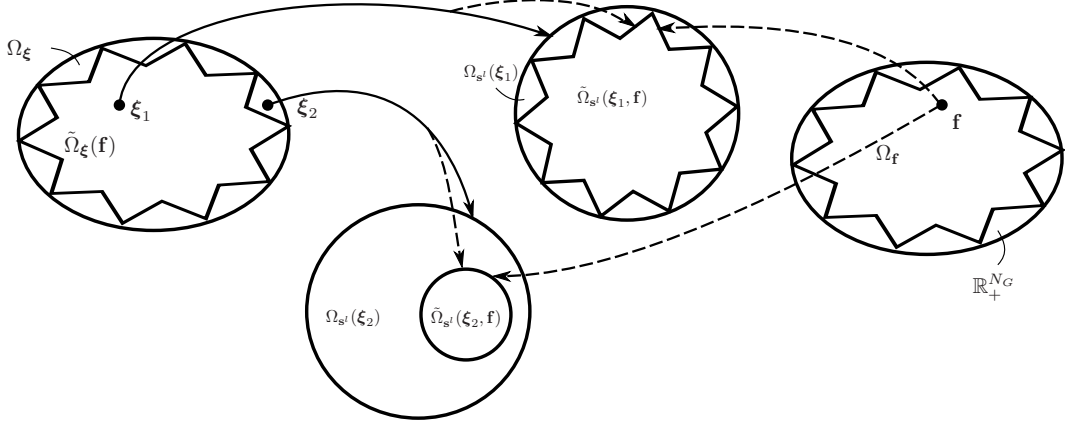


Figure 1: Relationship among definitions in Section 2.3. Solid arrows show the mapping from ξ to $\Omega_{s^l}(\xi)$, and dashed arrows show the mapping from (ξ, \mathbf{f}) to $\tilde{\Omega}_{s^l}(\xi, \mathbf{f})$. A star inscribed within an oval indicates the former set is dense within the latter.

$\tilde{\Omega}_{\xi}(\mathbf{f})$ depending on \mathbf{f} , and Proposition 3.3 implies $\tilde{\Omega}_{\xi}(\mathbf{f})$ is always dense in Ω_{ξ} . Informally, while the parameters in Ω guarantees (3) is feasible and \mathcal{OPF} is thereby well-defined, the parameters in $\tilde{\Omega}$ also guarantee that (3) has independent binding constraints and \mathcal{OPF} is singleton-valued. In the next section, we will further show \mathcal{OPF} is differentiable when $(\mathbf{f}, \xi, \mathbf{s}^l) \in \tilde{\Omega}$. Since all the sets that imply “good” properties ($\Omega_{\mathbf{f}}, \tilde{\Omega}_{s^l}, \tilde{\Omega}_{\xi}$) are dense with respect to the corresponding whole sets of interest ($\mathbb{R}_+^{NG}, \Omega_{s^l}, \Omega_{\xi}$), one can always perturb the parameters to endow \mathcal{OPF} with these desirable properties.

4 On the OPF Derivative

In this section we show that \mathcal{OPF} is differentiable almost everywhere. We also provide an equivalent perspective from which to view the derivative (Jacobian matrix) of \mathcal{OPF} in terms of binding constraints, and derive its closed form expression.³

4.1 Existence

Before deriving the expressions for the \mathcal{OPF} derivative, it is necessary to guarantee that the operator is in fact differentiable. The following lemma proposed in [11] and [12] gives the sufficient condition of differentiability. We rephrase the lemma as follows.

³A word on notation is in order here. We denote the derivative of x with respect to y by $\partial_y x$, however in some cases when there are complex dependencies on y we will use $\frac{\partial x}{\partial y}$. In Section 5 when we deal with derivatives of conic programs we use the notationally lighter differential operator \mathbf{D} .

Lemma 4.1. Consider a generic optimization problem parametrized by Θ :

$$\underset{\mathbf{x} \in \mathbb{R}^n}{\text{minimize}} \quad f(\mathbf{x}; \Theta) \quad (6a)$$

$$\text{subject to} \quad g_i(\mathbf{x}; \Theta) \leq 0, i = 1, 2, \dots, m \quad (6b)$$

$$h_j(\mathbf{x}; \Theta) = 0, j = 1, 2, \dots, l. \quad (6c)$$

If $(\mathbf{x}^*, \boldsymbol{\eta}^*, \boldsymbol{\nu}^*)$ is the primal-dual optimal solution for some Θ_0 and satisfies:

- 1) \mathbf{x}^* is a locally unique primal solution.
- 2) f, g_i, h_j are twice continuously differentiable in \mathbf{x} and differentiable in Θ .
- 3) The gradients $\nabla g_i(\mathbf{x}^*)$ for binding inequality constraints and $\nabla h_j(\mathbf{x}^*)$ for equality constraints are independent.
- 4) Strict complementary slackness holds, i.e., $g_i(\mathbf{x}^*) = 0 \Rightarrow \boldsymbol{\eta}_i > 0$.

Then the local derivative $\partial_{\Theta} \mathbf{x}^*$ exists at Θ_0 , and the set of binding constraints is unchanged in a small neighborhood of Θ_0 .

This leads to the following Theorem.

Theorem 4.2. Under Assumption 2 and Assumption 3, for $\mathbf{s}^l \in \tilde{\Omega}_{\mathbf{s}^l}$, the derivative $\partial_{\mathbf{s}^l} \mathcal{OPF}(\mathbf{s}^l)$ always exists, and the set of binding constraints stay unchanged in some neighborhood of \mathbf{s}^l .

Proof. By checking the conditions 1-4 in Lemma 4.1, the proof is established. \blacksquare

Having established existence of the derivative of \mathcal{OPF} we are now ready to study the associated Jacobian matrix.

4.2 Jacobian Matrix

In this subsection, we will derive the Jacobian matrix of the \mathcal{OPF} operator. The Jacobian is an important tool in sensitivity analysis as it provides the best linear approximation of an operator from input to output space. The results of the previous section ensure that the partial derivatives exist almost everywhere. Let

$$\mathbf{J}(\mathbf{s}^l; \mathbf{f}, \boldsymbol{\xi}) := \partial_{\mathbf{s}^l} \mathcal{OPF}(\mathbf{s}^l) \quad (7)$$

for $(\mathbf{f}, \boldsymbol{\xi}, \mathbf{s}^l) \in \tilde{\Omega}$ denote the Jacobian of \mathcal{OPF} . To reduce the notational burden, we will simply use \mathbf{J} or $\mathbf{J}(\mathbf{s}^l)$ for short when the value of $(\mathbf{f}, \boldsymbol{\xi}, \mathbf{s}^l)$ or $(\mathbf{f}, \boldsymbol{\xi})$ is clear from context. Suppose at point \mathbf{s}^l , the set of generators corresponding to binding inequalities is $\mathcal{S}_G \subseteq \mathcal{V}_G$, while the set of branches corresponding to binding inequalities is $\mathcal{S}_B \subseteq \mathcal{E}$. By Proposition 3.3 and Assumption 3, we have $|\mathcal{S}_G| + |\mathcal{S}_B| = N_G - 1$. As Lemma 4.1 implies that generators \mathcal{S}_G

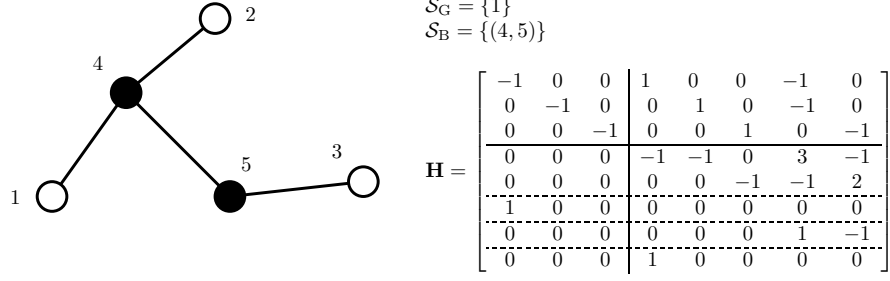


Figure 2: In the above 5-bus network, white and black nodes denote generators and loads, respectively. Assume generator 1 is a binding generator and branch (4, 5) is a binding branch. The \mathbf{H} matrix for this example is given in the figure.

and branches \mathcal{S}_B still correspond to binding constraints near \mathbf{s}^l , there is a local relationship between $\mathbf{s}^g = \mathcal{OPF}(\mathbf{s}^l)$ and \mathbf{s}^l :

$$\mathbf{H} \cdot \begin{bmatrix} \mathbf{s}^g \\ \boldsymbol{\theta} \end{bmatrix} = \begin{bmatrix} \mathbf{0}^{N_G \times 1} \\ -\mathbf{s}^l \\ \gamma^\top \boldsymbol{\xi} \\ 0 \end{bmatrix}, \quad \mathbf{H} := \left[\begin{array}{c|c} -\mathbf{I}^{N_G} & \mathbf{I}_{\mathcal{V}_G}^N \cdot \mathbf{CBC}^\top \\ \hline \mathbf{0}^{N_L \times N_G} & \mathbf{I}_{\mathcal{V}_L}^N \cdot \mathbf{CBC}^\top \\ \mathbf{I}_{\mathcal{S}_G}^{N_G} & \mathbf{0}^{|\mathcal{S}_G| \times N} \\ \mathbf{0}^{|\mathcal{S}_B| \times N_G} & \mathbf{I}_{\mathcal{S}_B}^E \cdot \mathbf{BC}^\top \\ \hline \mathbf{0}^{1 \times N_G} & \mathbf{e}_1^\top \end{array} \right]. \quad (8)$$

One example of \mathbf{H} is given in Fig. 2. On the right hand side, $\gamma \in \mathbb{R}^{(2N_G+2E) \times (N_G-1)}$ and each column of γ is a base vector such that $\gamma^\top \boldsymbol{\xi}$ gives the capacity limits that binding generations and branch power flows hit (similar as in Appendix C). By Corollary 3.5, the first $N + N_G - 1$ rows of \mathbf{H} are independent, and clearly the last row $[\mathbf{0}, \mathbf{e}_1^\top]$ does not depend on the first $N + N_G - 1$ rows. Hence \mathbf{H} is invertible, and using the block matrix inversion formula, we have

$$\begin{bmatrix} \mathbf{s}^g \\ \boldsymbol{\theta} \end{bmatrix} = \mathbf{H}^{-1} \begin{bmatrix} \mathbf{0}^{N_G \times 1} \\ -\mathbf{s}^l \\ \gamma^\top \boldsymbol{\xi} \\ 0 \end{bmatrix} = \begin{bmatrix} * & \mathbf{H}_1 \\ * & * \end{bmatrix} \begin{bmatrix} \mathbf{0}^{N_G \times 1} \\ -\mathbf{s}^l \\ \gamma^\top \boldsymbol{\xi} \\ 0 \end{bmatrix} \quad (9)$$

with

$$\mathbf{H}_1 = \mathbf{I}_{\mathcal{V}_G}^N \mathbf{CBC}^\top (\mathbf{R}(\mathcal{S}_G, \mathcal{S}_B)^\top)^{-1}, \quad \mathbf{R}(\mathcal{S}_G, \mathcal{S}_B)^\top := \begin{bmatrix} \mathbf{I}_{\mathcal{V}_L}^N \mathbf{CBC}^\top \\ \mathbf{I}_{\mathcal{S}_G}^N \mathbf{CBC}^\top \\ \mathbf{I}_{\mathcal{S}_B}^E \mathbf{BC}^\top \\ \mathbf{e}_1^\top \end{bmatrix}. \quad (10)$$

Recall (7) and the fact that the value of \mathcal{OPF} is \mathbf{s}^g in (9), so the Jacobian matrix \mathbf{J} is

$$\mathbf{J} = -\mathbf{H}_1 (\mathbf{I}_{[N_L]}^N)^\top. \quad (11)$$

It is worth noting that the value of \mathbf{J} computed via (8)-(11) depends on knowing the binding constraints \mathcal{S}_G and \mathcal{S}_B for given $(\mathbf{f}, \boldsymbol{\xi}, \mathbf{s}^l)$. We abuse notation slightly and let $\mathbf{J}(\mathbf{s}^l; \mathbf{f}, \boldsymbol{\xi})$ be the Jacobian matrix when $(\mathbf{f}, \boldsymbol{\xi}, \mathbf{s}^l) \in \tilde{\Omega}$ is known and let $\mathbf{J}(\mathcal{S}_G, \mathcal{S}_B)$ be the Jacobian matrix when $(\mathcal{S}_G, \mathcal{S}_B)$ is known. When it is clear from context or not relevant we simply use \mathbf{J} .

4.3 Codomain of OPF Derivative

The previous subsection has shown that the value of $\mathbf{J}(\mathbf{s}^l; \mathbf{f}, \boldsymbol{\xi})$ is equivalent to $\mathbf{J}(\mathcal{S}_G, \mathcal{S}_B)$ for certain choice of \mathcal{S}_G and \mathcal{S}_B . The following theorem also implies the equivalence between the codomain of $\mathbf{J}(\mathbf{s}^l; \mathbf{f}, \boldsymbol{\xi})$ and $\mathbf{J}(\mathcal{S}_G, \mathcal{S}_B)$.

Theorem 4.3.

$$\begin{aligned} & \{\mathbf{J}(\mathbf{s}^l; \mathbf{f}, \boldsymbol{\xi}) \mid (\mathbf{f}, \boldsymbol{\xi}, \mathbf{s}^l) \in \tilde{\Omega}\} \\ &= \{\mathbf{J}(\mathcal{S}_G, \mathcal{S}_B) \mid \mathcal{S}_G \in \mathcal{V}_G, \mathcal{S}_B \in \mathcal{E}, |\mathcal{S}_G| + |\mathcal{S}_B| = N_G - 1, \mathcal{S}_G \perp \mathcal{S}_B\}. \end{aligned} \quad (12)$$

Here, we use $\mathcal{S}_G \perp \mathcal{S}_B$ to denote that in Eq. (3), all the inequality constraints corresponding to \mathcal{S}_G and \mathcal{S}_B , as well as equality constraints, are independent of each other. It is worth noting that the left hand side of Eq. (12) is induced by the DC-OPF problem and hence involves physical parameters such as the cost function, generation and load. The right hand side, however, purely depends on the graph topology. Theorem 4.3 shows the equivalence between the value ranges of $\mathbf{J}(\mathbf{s}^l)$ and $\mathbf{J}(\mathcal{S}_G, \mathcal{S}_B)$.

We first provide the following lemmas in order to build up to the final proof for Theorem 4.3. We defer their proofs to Appendix D.

Lemma 4.4. *For any $\mathcal{S}_G \in \mathcal{V}_G, \mathcal{S}_B \in \mathcal{E}$ such that $|\mathcal{S}_G| + |\mathcal{S}_B| = N_G - 1$ and $\mathcal{S}_G \perp \mathcal{S}_B$, there exist $(\mathbf{f}_*, \boldsymbol{\xi}_*, \mathbf{s}_*^l) \in \Omega$ such that (3) has unique solution and all the binding constraints at the solution point exactly correspond to \mathcal{S}_G and \mathcal{S}_B .*

Proof. See Appendix D. ■

Lemma 4.5. *For any $\mathcal{S}_G \in \mathcal{V}_G, \mathcal{S}_B \in \mathcal{E}$ such that $|\mathcal{S}_G| + |\mathcal{S}_B| = N_G - 1$ and $\mathcal{S}_G \perp \mathcal{S}_B$, there exist $\mathbf{f}_{**} \in \Omega_{\mathbf{f}}, \boldsymbol{\xi}_{**} \in \tilde{\Omega}_{\boldsymbol{\xi}}(\mathbf{f}_{**})$ and an open ball $W \subseteq \tilde{\Omega}_{\mathbf{s}^l}(\boldsymbol{\xi}_{**}, \mathbf{f}_{**})$ such that all the binding constraints exactly correspond to \mathcal{S}_G and \mathcal{S}_B whenever $\mathbf{s}^l \in W$.*

Proof. See Appendix D. ■

Now we have all the ingredients for proving Theorem 4.3.

Proof.(Theorem 4.3) For any $(\mathbf{f}, \boldsymbol{\xi}, \mathbf{s}^l) \in \tilde{\Omega}$, by definition the binding constraints \mathcal{S}_G and \mathcal{S}_B must satisfy $|\mathcal{S}_G| + |\mathcal{S}_B| = N_G - 1$ and $\mathcal{S}_G \perp \mathcal{S}_B$. Thus the left hand side of (12) is a subset of the right hand side of (12). As for the opposite direction, Lemma 4.5 implies for any $(\mathcal{S}_G, \mathcal{S}_B)$ such that $|\mathcal{S}_G| + |\mathcal{S}_B| = N_G - 1$ and $\mathcal{S}_G \perp \mathcal{S}_B$ we can always find $(\mathbf{f}, \boldsymbol{\xi}, \mathbf{s}^l) \in \tilde{\Omega}$ whose associated binding constraints exactly correspond to $(\mathcal{S}_G, \mathcal{S}_B)$. Hence the right hand side of (12) is also a subset of the left hand side. ■

The result of Theorem 4.3 also indicates there exists a surjection from $\tilde{\Omega}$ to the set $\{(\mathcal{S}_G, \mathcal{S}_B) \mid |\mathcal{S}_G| + |\mathcal{S}_B| = N_G - 1, \mathcal{S}_G \perp \mathcal{S}_B\}$ and the derivative of the operator (depending on the parameters) and the Jacobian matrix (depending on the binding constraints combination) take the same value under such surjection. If one is only interested in the codomain of $\mathbf{J}(\mathbf{s}^l; \mathbf{f}, \boldsymbol{\xi})$ such as the worst-case analysis instead of the value at a specific point, then $\mathbf{J}(\mathbf{s}^l; \mathbf{f}, \boldsymbol{\xi})$ and $\mathbf{J}(\mathcal{S}_G, \mathcal{S}_B)$ may be used interchangeably. One benefit of studying $\mathbf{J}(\mathcal{S}_G, \mathcal{S}_B)$ is it has a closed form expression and only depends on the graph topology of the system.

5 Computation

In the previous section, we provided a closed form expression for the Jacobian $\mathbf{J} = \partial_{\mathbf{s}^l} \mathcal{OPF}(\mathbf{s}^l)$ which depends on the binding generators and branches. This expression will be very useful in shedding light on further properties of the sensitivity of the DC-OPF problem. For instance, it helps us study the OPF sensitivity bounds in the “worst case”, which provides privacy guarantees when releasing power flow data [39]. On the other hand, the method above is restricted to the DC OPF problems and only reflects how the optimal solution changes when \mathbf{s}^l is perturbed.

In this section, we will show how recent results on conic problem differentiation can be applied to the OPF operator, specifically in the case when one simply focuses on evaluating a derivative at a given operating point. This method could provide the derivative of the optimal solution with respect to different system parameters, and could also be generalized to other power flow models. For example, in Section 5.3 we describe how these results can be applied to an AC OPF problem when a semidefinite relaxation of the power flow equations is considered. In this setting we are unable to guarantee the existence of the derivative and we leave this to future work.

Here we provide a numerical method to compute derivatives of \mathcal{OPF} with respect to arbitrary problem data in (3). In Section 5.1 we first rephrase a recent result [1] which is developed for a general conic program formulation. We then in Section 5.2 and Section 5.3 reformulate the DC and AC OPF problems into such conic program formulation so the theory can directly apply.

5.1 Differentiating a General Conic Program

The method of computation we pursue largely follows that presented in [1] which considers general convex conic optimization problems that are solved using the homogenous self-dual embedding framework [36, 29]. Consider a standard primal-dual pair written in conic form:

$$\begin{array}{ll}
 \text{minimize}_{\mathbf{x}, \mathbf{s}} & \mathbf{c}^\top \mathbf{x} \\
 \text{(P) subject to} & \mathbf{A}\mathbf{x} + \mathbf{s} = \mathbf{b} \\
 & (\mathbf{x}, \mathbf{s}) \in \mathbb{R}^n \times \mathcal{K},
 \end{array}
 \qquad
 \begin{array}{ll}
 \text{minimize}_{\mathbf{y}, \mathbf{r}} & \mathbf{b}^\top \mathbf{y} \\
 \text{(D) subject to} & \mathbf{A}^\top \mathbf{y} + \mathbf{c} = \mathbf{r} \\
 & (\mathbf{r}, \mathbf{y}) \in \{0\}^n \times \mathcal{K}^*.
 \end{array}$$

In this setting the problem data consists of the triple $(\mathbf{A}, \mathbf{b}, \mathbf{c}) \in \mathbb{R}^{m \times n} \times \mathbb{R}^m \times \mathbb{R}^n$. The primal variable is $\mathbf{x} \in \mathbb{R}^n$, the primal slack variable is $\mathbf{s} \in \mathbb{R}^m$, and the dual variable is

$\mathbf{y} \in \mathbb{R}^m$, with $\mathbf{r} \in \mathbb{R}^n$ the dual slack variable. The set \mathcal{K} is a non-empty, closed, convex cone with \mathcal{K}^* its dual. Linear programming and semi-definite programming both fall into this class of conic problems by setting \mathcal{K} to be the positive orthant or the semi-definite cone.

The KKT conditions for primal-dual optimality are $\mathbf{A}\mathbf{x} + \mathbf{s} = \mathbf{b}$, $\mathbf{A}^\top \mathbf{y} + \mathbf{c} = \mathbf{r}$, $\mathbf{r} = \mathbf{0}$, $\mathbf{s} \in \mathcal{K}$, $\mathbf{y} \in \mathcal{K}^*$, and $\mathbf{s}^\top \mathbf{y} = 0$. The homogenous self-dual embedding formulation is expressed as

$$\begin{aligned} & \text{find } (\mathbf{u}, \mathbf{v}) \\ & \text{subject to } \mathbf{v} = \mathbf{Q}\mathbf{u} \\ & (\mathbf{u}, \mathbf{v}) \in \mathcal{C} \times \mathcal{C}^* \end{aligned} \tag{13}$$

with cones $\mathcal{C} = \mathbb{R}^n \times \mathcal{K}^* \times \mathbb{R}_+$ and its dual $\mathcal{C}^* = \{0\}^n \times \mathcal{K} \times \mathbb{R}_+$. The variables \mathbf{u} and \mathbf{v} correspond to variables in (P) and (D) and two augmented variables κ and τ , and satisfy the mapping:

$$\underbrace{\begin{bmatrix} \mathbf{r} \\ \mathbf{s} \\ \kappa \end{bmatrix}}_{\mathbf{v}} = \underbrace{\begin{bmatrix} \mathbf{0} & \mathbf{A}^\top & \mathbf{c} \\ -\mathbf{A} & \mathbf{0} & \mathbf{b} \\ -\mathbf{c}^\top & -\mathbf{b}^\top & 0 \end{bmatrix}}_{\mathbf{Q}} \underbrace{\begin{bmatrix} \mathbf{x} \\ \mathbf{y} \\ \tau \end{bmatrix}}_{\mathbf{u}}, \quad (\tau, \kappa) \in \mathbb{R}_+ \times \mathbb{R}_+,$$

which is exactly the affine constraint in (13). Using Minty's parametrization [31], we let $\mathbf{z} \in \mathbb{R}^{n+m+1}$ denote $\mathbf{u} - \mathbf{v}$, giving $\mathbf{u} = \mathcal{P}_{\mathcal{C}}\mathbf{z}$, and $\mathbf{v} = -\mathcal{P}_{-\mathcal{C}^*}\mathbf{z}$. Now reformulate (13) in terms of \mathbf{z} as

$$\begin{aligned} & \text{find } \mathbf{z} = (\mathbf{z}_1 \in \mathbb{R}^n, \mathbf{z}_2 \in \mathbb{R}^m, \mathbf{z}_3 \in \mathbb{R}) \in \mathbb{R}^{n+m+1} \\ & \text{subject to } -\mathcal{P}_{-\mathcal{C}^*}\mathbf{z} = \mathbf{Q}\mathcal{P}_{\mathcal{C}}\mathbf{z} \\ & \mathbf{z}_3 > 0. \end{aligned} \tag{14}$$

The *solution map* is defined as $\mathcal{S} : \mathbb{R}^{m \times n} \times \mathbb{R}^m \times \mathbb{R}^n \rightarrow \mathbb{R}^{2m+n}$ which “pushes” the problem data $(\mathbf{A}, \mathbf{b}, \mathbf{c})$ through optimization problem (13) to return $(\mathbf{x}, \mathbf{y}, \mathbf{s})$ – the primal-dual solutions. As a functional, we can write $\mathcal{S} = \psi \circ \phi \circ Q$. The function Q constructs the skew-symmetric matrix \mathbf{Q} from $(\mathbf{A}, \mathbf{b}, \mathbf{c})$. The mapping $\phi : \mathcal{Q} \rightarrow \mathbb{R}^{n+m+1}$ maps from the space of skew-symmetric matrices to solution \mathbf{z} of the self-dual embedding Eq. (14). Finally, $\psi : \mathbb{R}^{n+m+1} \rightarrow \mathbb{R}^n \times \mathbb{R}^m \times \mathbb{R}^m$ constructs the primal-dual solutions of (P) and (D) from the self-dual embedding solution, i.e. $(\mathbf{x}, \mathbf{y}, \mathbf{s}) = \psi(\mathbf{z})$ where

$$\psi(\mathbf{z}) = (\mathbf{z}_1, \mathcal{P}_{\mathcal{K}^*}\mathbf{z}_2, \mathcal{P}_{\mathcal{K}^*}\mathbf{z}_2 - \mathbf{z}_2)/\mathbf{z}_3$$

with \mathbf{z} a solution of the self-dual embedding Eq. (14).

The following result is taken from [1], it is essentially an application of the chain-rule and the implicit function theorem. Consider the perturbation in problem data, $(d\mathbf{A}, d\mathbf{b}, d\mathbf{c})$, and the derivative of the solution map, $\partial\mathcal{S}/\partial(\mathbf{A}, \mathbf{b}, \mathbf{c})$, then the perturbation on the primal-dual solutions is evaluated from

$$(d\mathbf{x}, d\mathbf{y}, d\mathbf{s}) = \frac{\partial\mathcal{S}(\mathbf{A}, \mathbf{b}, \mathbf{c})}{\partial(\mathbf{A}, \mathbf{b}, \mathbf{c})}(d\mathbf{A}, d\mathbf{b}, d\mathbf{c}) = \frac{\partial\psi(\mathbf{z})}{\partial\mathbf{z}} \frac{\partial\phi(\mathbf{Q})}{\partial\mathbf{Q}} \frac{\partial Q(\mathbf{A}, \mathbf{b}, \mathbf{c})}{\partial(\mathbf{A}, \mathbf{b}, \mathbf{c})}(d\mathbf{A}, d\mathbf{b}, d\mathbf{c}).$$

To evaluate the values of $(d\mathbf{x}, d\mathbf{y}, d\mathbf{s})$, we first derive the expression for $d\mathbf{z}$ and then recover $(d\mathbf{x}, d\mathbf{y}, d\mathbf{s})$ from $d\mathbf{z}$. Numerically, [1] show that $d\mathbf{z} = -\mathbf{M}^{-1}\mathbf{g}$, where

$$\begin{aligned}\mathbf{M} &= ((\mathbf{Q} - \mathbf{I})D\mathcal{P}_{\mathcal{C}}\mathbf{z} + \mathbf{I})/\mathbf{z}_3 \\ \mathbf{g} &= d\mathbf{Q}\mathcal{P}_{\mathcal{C}}(\mathbf{z}/\mathbf{z}_3) \\ d\mathbf{Q} &= \begin{bmatrix} \mathbf{0} & d\mathbf{A}^\top & d\mathbf{c} \\ -d\mathbf{A} & \mathbf{0} & d\mathbf{b} \\ -d\mathbf{c}^\top & -d\mathbf{b}^\top & \mathbf{0} \end{bmatrix}.\end{aligned}\tag{15}$$

Here we use D instead of ∂ to denote the derivative of an operator when the arguments are clear from context. Note that for large systems it may be preferable to not invert \mathbf{M} and instead solve a least squares problem. Finally, partition $d\mathbf{z}$ conformally as $(d\mathbf{z}_1, d\mathbf{z}_2, d\mathbf{z}_3)$ and compute

$$\begin{bmatrix} d\mathbf{x} \\ d\mathbf{y} \\ d\mathbf{s} \end{bmatrix} = \begin{bmatrix} d\mathbf{z}_1 - (d\mathbf{z}_3)\mathbf{x} \\ (D\mathcal{P}_{\mathcal{K}^*}(\mathbf{z}_2))d\mathbf{z}_2 - (d\mathbf{z}_3)\mathbf{y} \\ (D\mathcal{P}_{\mathcal{K}^*}(\mathbf{z}_2))d\mathbf{z}_2 - d\mathbf{z}_2 - (d\mathbf{z}_3)\mathbf{s} \end{bmatrix}.\tag{16}$$

The method outlined above provides us with more information than we have considered to this point. Specifically, it leverages information about the primal and dual conic forms and provides derivative information with respect to all problem data rather than just load changes.

5.2 DC Optimal Power Flow

The DC Optimal power flow problem (3) can easily be written in the form (P) by introducing the appropriate slack variables and taking $\mathcal{K} = \{0\}^{N+1} \times \mathbb{R}_+^{2N_G+2E}$:

$$\begin{aligned}\text{minimize}_{\mathbf{x} := [(\mathbf{s}^g)^\top, \boldsymbol{\theta}^\top]^\top, \mathbf{s}} \quad & [\mathbf{f}^\top, \mathbf{0}^\top]\mathbf{x}\end{aligned}\tag{17a}$$

$$\text{subject to} \quad \begin{bmatrix} \mathbf{A}_{\text{eq}} \\ \mathbf{A}_{\text{in}} \end{bmatrix} \mathbf{x} + \mathbf{s} = \begin{bmatrix} \mathbf{b}_{\text{eq}} \\ \mathbf{b}_{\text{in}} \end{bmatrix}\tag{17b}$$

$$(\mathbf{x}, \mathbf{s}) \in \mathbb{R}^{N_G+N} \times (\{0\}^{N+1} \times \mathbb{R}_+^{2N_G+2E})\tag{17c}$$

where $(\mathbf{A}_{\text{eq}}, \mathbf{A}_{\text{in}}, \mathbf{b}_{\text{eq}}, \mathbf{b}_{\text{in}})$ are as defined in Eq. (22). Noting that $\mathcal{K}^* = \mathbb{R}^{N+1} \times \mathbb{R}_+^{2N_G+2E}$.

Here we note that the derivative of the projection operator $D\mathcal{P}_{\mathcal{C}}$ appearing in Eq. (15) is decomposed as

$$D\mathcal{P}_{\mathbb{R}^{N_G+N}} \times D\mathcal{P}_{\mathbb{R}^{N+1}} \times D\mathcal{P}_{\mathbb{R}_+^{2N_G+2E}} \times D\mathcal{P}_{\mathbb{R}_+}$$

and $D\mathcal{P}_{\mathcal{K}^*}$ appearing in Eq. (16) is decomposed as

$$D\mathcal{P}_{\mathbb{R}^{N+1}} \times D\mathcal{P}_{\mathbb{R}_+^{2N_G+2E}}.$$

Specifically, $D\mathcal{P}_{\mathbb{R}_+}$ is differentiable everywhere but at $\{0\}$, elsewhere

$$D\mathcal{P}_{\mathbb{R}_+}\mathbf{x} = \frac{1}{2}(\text{sign}(\mathbf{x}) + 1).$$

5.3 AC Optimal Power Flow

In this subsection we briefly outline how the methods described in the previous section extend seamlessly to a semidefinite programming based relaxation of the AC optimal power flow problem. Unlike with the DC case, we make no claim as to when the derivatives are guaranteed to exist.

For AC OPF problems, the loads \mathbf{s}^l and generations \mathbf{s}^g become complex numbers, where the real part denotes the real power and the imaginary part denotes the reactive power. In [22], the *bus injection* AC OPF problem is formulated as

$$\begin{aligned} & \underset{\mathbf{W} \in \mathbb{S}_N^+}{\text{minimize}} && \text{tr}(\mathbf{C}_0 \mathbf{W}) \end{aligned} \quad (18a)$$

$$\text{subject to} \quad \text{tr}(\mathbf{C}_i \mathbf{W}) \leq \mathbf{b}_i \quad i = 1, 2, \dots, m \quad (18b)$$

$$\text{rank}(\mathbf{W}) = 1 \quad (18c)$$

where \mathbb{S}_N^+ is the space of all the $N \times N$ positive semidefinite Hermitian matrices. Matrices $\mathbf{C}_i (i = 0, 1, \dots, m)$ are determined by the power system parameters such as admittances and the network topology. The values $\mathbf{b}_i (i = 1, \dots, m)$ depend on both the load profile \mathbf{s}^l and system capacity limits, and \mathbf{b} is linear in \mathbf{s}^l . The optimal generation $\mathbf{s}^g = \mathcal{OPF}(\mathbf{s}^l)$ is linear in the optimal solution \mathbf{W}^* of Eq. (18).⁴ The task is to now derive the derivative $d\mathbf{s}^g$ with respect to the perturbation \mathbf{s}^l . Following the same arguments as the previous section, all that remains to be done is to numerically compute $d\mathbf{W}$ for perturbations to \mathbf{b} .

As (18) is non-convex and thereby computationally challenging, the semidefinite relaxation is always applied by dropping the non-convex rank constraint (18c). For radial networks (i.e., when \mathcal{G} is a tree), there are sufficient conditions under which the semidefinite relaxation is exact in the sense that it yields the same optimal solution as (18); see [23] and [27] for extensive references. The relaxed problem (18a)-(18b) is a semidefinite programming problem and thereby can be rewritten in the canonical form of a conic program as in (P) and (D). The same technique in Section 5.1 can be applied to numerically evaluate $d\mathbf{W}$ – the formulae for the derivative of the projection operator for the semidefinite cone can be found in [1] and [24]. It should be noted however, that perturbations to \mathbf{W} need not result in a rank-one solution.

6 Illustrative Examples

In this section, we use the IEEE 9-bus test network as an example to illustrate what the sets $(\Omega_f, \Omega_\xi, \tilde{\Omega}_\xi, \Omega_{s^l}, \tilde{\Omega}_{s^l})$ in Fig. 1 look like. The topology of the network is shown in Fig. 3. It has three generators (white circles) and 6 loads (black circles). The susceptances (edge weights) of power lines are taken from the MATPOWER toolbox [40]. The system parameters are provided in Table 1. The data for the capacity limits and the loads are either directly taken from MATPOWER or perturbed to satisfy our assumptions.

⁴Here we extend the notation \mathcal{OPF} as the mapping that returns the optimal \mathbf{s}^g for given \mathbf{s}^l based on the AC OPF problem.

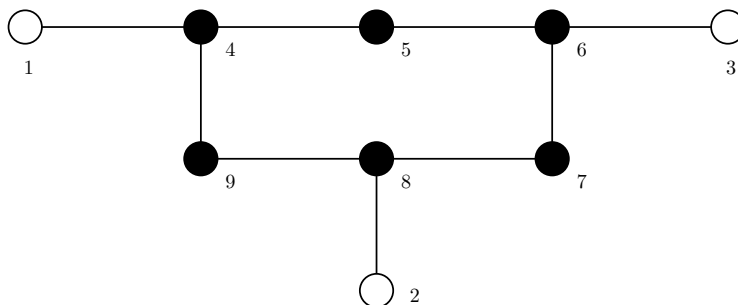


Figure 3: Diagram of IEEE 9-bus test network. Generators are represented by white circles, while load buses are colored in black.

Table 1: IEEE 9-bus Parameter Specification. The unit for the capacity limits and loads is 100 MW.

cost	\mathbf{f}_1				\mathbf{f}_2			\mathbf{f}_3		
	0.7191				0.5066			0.4758		
capacity limits	$i \in \mathcal{V}_G$		1		2			3		
	$\overline{\mathbf{s}}^g$		2.5679		3.0758			2.7743		
	$\underline{\mathbf{s}}^g$		0.1392		0.1655			0.1171		
	\mathcal{E}	(1, 4)	(4, 5)	(5, 6)	(3, 6)	(6, 7)	(7, 8)	(8, 9)	(4, 9)	
	$\overline{\mathbf{p}}$	2.571	2.503	1.528	3.005	1.510	2.582	2.532	2.595	
	$\underline{\mathbf{p}}$	-2.503	-2.544	-1.538	-3.077	-1.580	-2.519	-2.545	-2.565	
	Visualization: the upper and lower bounds for branch (2, 8)									
load	$i \in \mathcal{V}_L$		5		6		8		9	
	\mathbf{s}^l		0.90		10^{-10}		10^{-10}		1.25	
	Visualization: the loads of buses 4 and 7									

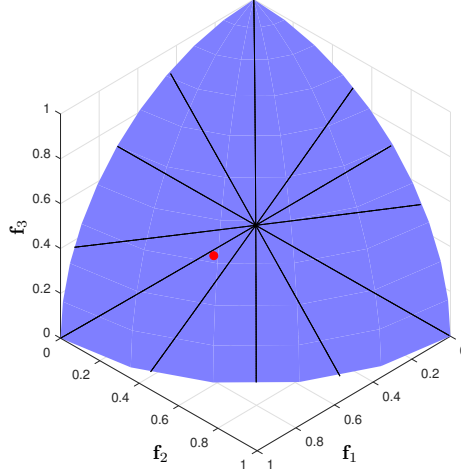


Figure 4: Region for the cost vector \mathbf{f} . Black lines denote the values of \mathbf{f} in $\mathbb{R}_+^{N_G} \setminus \Omega_{\mathbf{f}}$. The red dot denotes the cost vector as indicated in Table 1 and used throughout this example.

First, we visualize and illustrate the sets $\mathbb{R}_+^{N_G}$ and $\Omega_{\mathbf{f}}$ where the cost vector \mathbf{f} resides. As we ignore the trivial case when $\mathbf{f} = \mathbf{0}$, we restrict \mathbf{f} to the unit sphere for visual clarity. As a result, $\mathbb{R}_+^{N_G}$ is visualized by the blue region including the boundary and black curve segments shown in Fig. 4. The black curve segments represent the set of \mathbf{f} which may potentially make the OPF problem have multiple solutions or violate Eq. (5). Thereby the blue region excluding the black curve segments is the restriction of a subset of $\Omega_{\mathbf{f}}$ onto the unit sphere. Fig. 4 provides a visualization that $\Omega_{\mathbf{f}}$ is dense in $\mathbb{R}_+^{N_G}$ ($N_G = 3$ in this example). If the cost vector \mathbf{f} is randomly chosen in $\mathbb{R}_+^{N_G}$, then we will almost surely obtain a well-behaved \mathbf{f} not aligned with the black curves. In the rest of this example, we randomly pick $\mathbf{f} = [0.7191, 0.5066, 0.4758]^T$, which is shown in the ‘cost’ sector in Table 1, and visualized as the red point in Fig. 4.

We will now visualize the sets Ω_{ξ} and $\tilde{\Omega}_{\xi}(\mathbf{f})$ for our choice of \mathbf{f} , and illustrate how different points in those two sets endow the OPF problem with different properties. Consider that there are 3 generators and 9 branches in the network, and each generator and branch has both the upper and lower bounds for its generation and branch power flow, the vector ξ thus has 24 dimensions and it is clearly impractical for us to visualize the set in such high dimensional space. In order to make visualization possible, we fix all the capacity limits except for the power flow limits at branch (2, 8) as in Table 1. A positive power flow at branch (u, v) means that power is transmitted from u to v . Conversely, a negative value implies power is transmitted in the opposite direction. Fig. 5 shows when \mathbf{f} and other capacity limits are fixed, how the upper and lower bounds for branch (2, 8) affect the OPF operator. In other words, Fig. 5 visualizes a slice of sets Ω_{ξ} and $\tilde{\Omega}_{\xi}(\mathbf{f})$. The blue region, including the boundaries and black lines, is the slice of Ω_{ξ} . Picking any point in the blue region as the capacity limits for branch (2, 8), there exist some $\mathbf{s}^l > 0$ such that the constraints (3b)-(3e) are feasible. However, for some points on the black lines or boundaries, the associated set

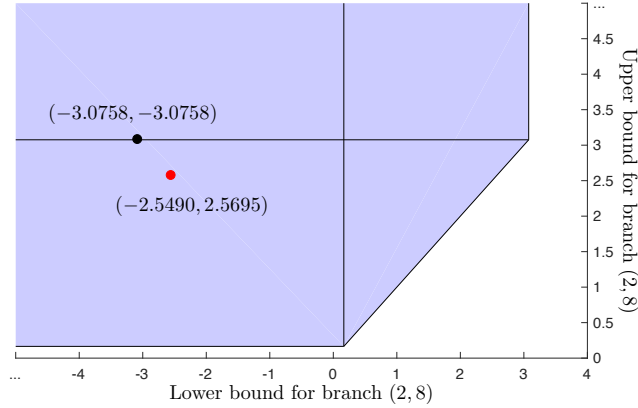
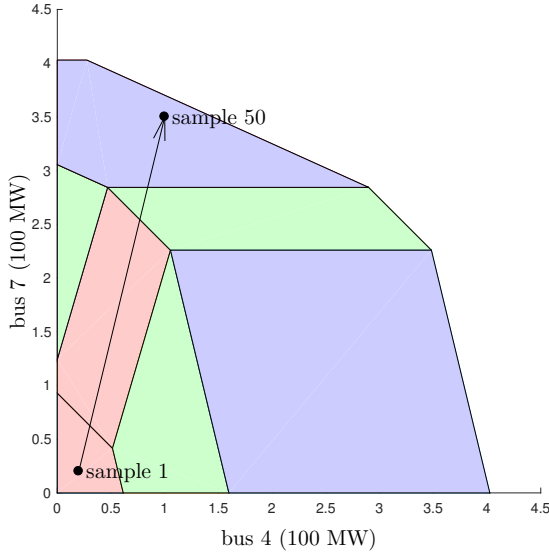


Figure 5: Feasibility region for the power flow limits at branch (2, 8). The polytope (including its boundaries and the black lines) is (a slice of) Ω_{ξ} . The set $\tilde{\Omega}_{\xi}(\mathbf{f})$ is given by the blue region excluding the black lines and boundaries.

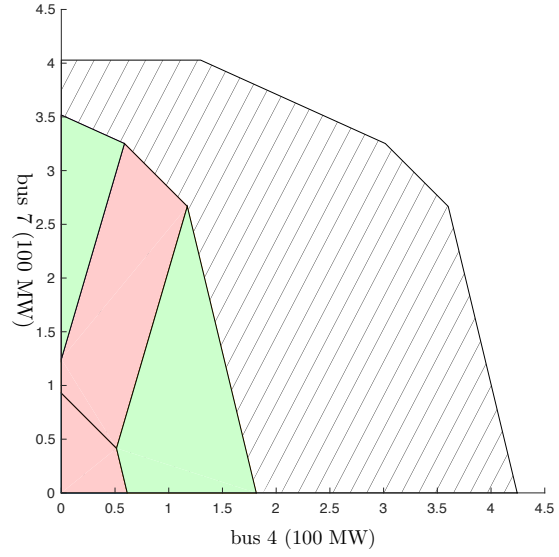
$\tilde{\Omega}_{s^l}(\xi, \mathbf{f})$ might be not dense in $\Omega_{s^l}(\xi)$. We collect all the points in the blue region excluding the black lines and boundaries to form a slice of $\tilde{\Omega}_{\xi}(\mathbf{f})$, which is dense in Ω_{ξ} . We now pick the red point in $\tilde{\Omega}_{\xi}(\mathbf{f})$ (not on the black lines) and the black point in $\Omega_{\xi} \setminus \tilde{\Omega}_{\xi}(\mathbf{f})$ (on the black line) as shown in Fig. 5, and will show their difference. Recall that in Fig. 1, we plot two points $\xi_1 \in \tilde{\Omega}_{\xi}(\mathbf{f})$ and $\xi_2 \in \Omega_{\xi} \setminus \tilde{\Omega}_{\xi}(\mathbf{f})$, so the red point visualizes ξ_1 while the black point visualizes ξ_2 .

First, we pick the red point in Fig. 5, i.e., set the lower and upper bounds for branch (2, 8) at $(-2.5490, 2.5695)$, respectively. Since it is difficult to visualize all 6 loads, we fix buses 5, 6, 8 and 9 as in Table 1, and visualize the region for buses 4 and 7 in Fig. 6a. The whole hexagon excluding the axes represents the slice of $\Omega_{s^l}(\xi)$, within which any point corresponds to a load profile which makes the OPF problem feasible. The whole region is further divided into seven colored subregions, and each of them refers to the set of load profiles under which the binding constraints of (3) do not change. In the interior of those subregions, there will be exactly $N_G - 1 = 2$ independent binding inequality constraints. Depending on the physical meaning of binding inequalities, we use three colors to distinguish different subregions. Red indicates two binding constraints refer to two binding generators, green indicates one generator and one branch are binding, and blue indicates two binding branches. Only the interior of those colored subregions contribute to the set $\tilde{\Omega}_{s^l}(\xi, \mathbf{f})$, which guarantees the number of and independence among all the binding constraints. The operator \mathcal{OPF} is also guaranteed to be differentiable when the loads are picked in $\tilde{\Omega}_{s^l}(\xi, \mathbf{f})$, and here the Jacobian matrix is given in Section 4.2 in a closed form. From Fig. 6a we can see that when the red point is picked, the interior of all the subregions (i.e., $\tilde{\Omega}_{s^l}(\xi, \mathbf{f})$) is dense in the whole hexagon (i.e., $\Omega_{s^l}(\xi)$).

Next, we pick the black point in Fig. 5, i.e., set the lower and upper bounds for branch (2, 8) at $(-3.0758, 3.0758)$. In this case, the whole hexagon contains a large chunk of shaded area. For the load profile in the shaded area, there might be more than $N_G - 1 = 2$ binding



(a) When ξ is selected at the red point.



(b) When ξ is selected at the black point.

Figure 6: Region for the loads (bus 4 and bus 7). inequality constraints, and all the binding constraints are not independent any more. The Jacobian matrix we derived in Section 4.2 is no longer valid. As the shaded area is non-negligible, the interior of all the subregions is not dense in the whole hexagon any more.

Fortunately, both our theoretical proof and Fig. 5 show that for almost all the capacity limits, they will behave like the red point in the above example and guarantee the independence among binding constraints for almost all the feasible load profiles.

Finally, we consider a path in Fig. 6a which goes through four different subregions, and pick 50 sample points along the path. Each sample point corresponds to a specific load profile for the power system. In Fig. 7, we show how the optimal generations and costs change for those 50 sample load profiles. In each subregion, the gradient of the optimal solution stays unchanged until the load profile enters a new subregion.

7 Conclusion

We presented an approach for analyzing a linear program that solves the DC optimal power flow problem based on operator theoretic techniques. Sets were defined upon which the OPF operator has a unique solution, is continuous, induce independent binding constraints, and the derivative exists (almost everywhere). Two equivalent perspectives on Jacobian matrix were given. The first was from the problem data and the second from knowledge of the binding constraints. A closed form expression of the Jacobian matrix is derived in terms of the binding constraints sets. Finally a numerical method based upon differentiating the solution map of a homogeneous self-dual conic program was described.

It is hoped that this formulation will provide practitioners with new tools for analyzing

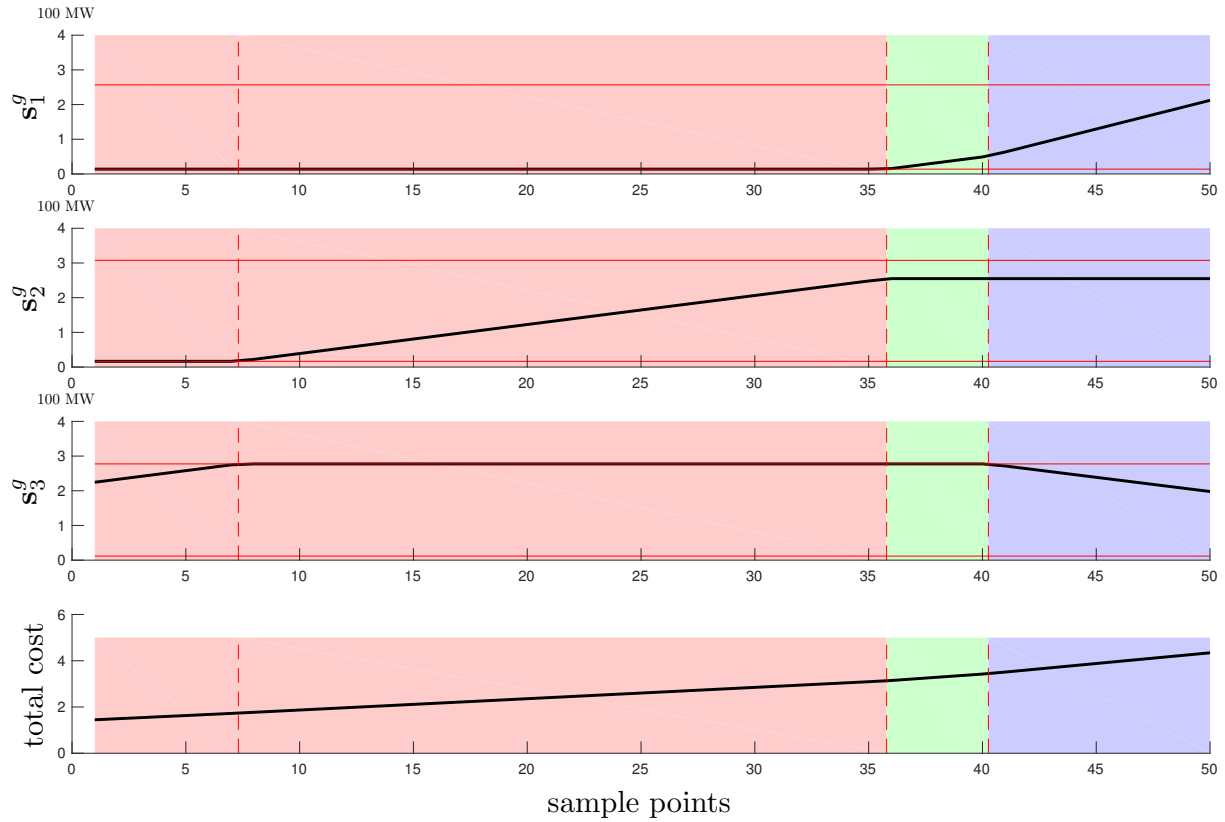


Figure 7: Optimal generations and costs for different sample load profiles along the path plotted in Fig. 6a. The solid red horizontal lines indicate the upper and lower bounds for the generation.

the robustness of their networks. Simultaneously, it opens up many interesting theoretical questions. In particular, studying AC optimal power flow problems from this perspective seems like a promising line of research. We are currently investigating how to compute the worst-case sensitivity of the DC-optimal power flow problem as this appears in a diverse range of applications including differential privacy, real-time optimal power flow problems, and locational marginal pricing.

Acknowledgements

This work was funded by NSF grants CCF 1637598, CPS 1739355, and ECCS 1619352, PNNL grant 424858, ARPA-E NODES through grant DE-AR0000699, and the ARPA-E GRID DATA program.

References

- [1] A. AGRAWAL, S. BARRATT, S. BOYD, E. BUSSETI, AND W. M. MOURSI, *Differentiating through a conic program*, arXiv preprint arXiv:1904.09043, (2019).
- [2] B. AMOS AND J. Z. KOLTER, *Optnet: Differentiable optimization as a layer in neural networks*, in Proceedings of the 34th International Conference on Machine Learning-Volume 70, 2017, pp. 136–145.
- [3] J. ANDERSON, F. ZHOU, AND S. H. LOW, *Disaggregation for networked power systems*, in 2018 Power Systems Computation Conference (PSCC), IEEE, 2018, pp. 1–7.
- [4] A. BEN-TAL, L. E. GHAOUI, AND A. NEMIROVSKI, *Robust optimization*, vol. 28, Princeton University Press, 2009.
- [5] D. BERTSIMAS, D. B. BROWN, AND C. CARAMANIS, *Theory and applications of robust optimization*, SIAM review, 53 (2011), pp. 464–501.
- [6] D. BERTSIMAS AND J. N. TSITSIKLIS, *Introduction to linear optimization*, vol. 6, Athena Scientific Belmont, MA, 1997.
- [7] S. BOYD AND L. VANDENBERGHE, *Convex optimization*, Cambridge university press, 2004.
- [8] J. CARPENTIER, *Contribution to the economic dispatch problem*, Bulletin de la Societe Francoise des Electriciens, 3 (1962), pp. 431–447.
- [9] G. DANTZIG, *Linear programming and extensions*, Princeton university press, 2016.
- [10] W. H. DOMMEL AND W. F. TINNEY, *Optimal power flow solutions*, IEEE Transactions on power apparatus and systems, (1968), pp. 1866–1876.

- [11] A. V. FIACCO, *Sensitivity analysis for nonlinear programming using penalty methods*, Mathematical programming, 10 (1976), pp. 287–311.
- [12] A. V. FIACCO, *Introduction to sensitivity and stability analysis in nonlinear programming*, (1983).
- [13] S. FRANK AND S. REBENNACK, *An introduction to optimal power flow: Theory, formulation, and examples*, IIE Transactions, 48 (2016), pp. 1172–1197.
- [14] S. FRANK, I. STEPONAVICE, AND S. REBENNACK, *Optimal power flow: a bibliographic survey i*, Energy Systems, 3 (2012), pp. 221–258.
- [15] X. GENG AND L. XIE, *Learning the LMP-load coupling from data: A support vector machine based approach*, IEEE Transactions on Power Systems, 32 (2016), pp. 1127–1138.
- [16] P. R. GRIBIK, D. SHIRMOHAMMADI, S. HAO, AND C. L. THOMAS, *Optimal power flow sensitivity analysis*, IEEE Transactions on Power Systems, 5 (1990), pp. 969–976.
- [17] J. GUDDAT, F. G. VAZQUEZ, AND H. T. JONGEN, *Parametric optimization: singularities, path following and jumps*, Springer, 1990.
- [18] D. P. HEYMAN AND M. J. SOBEL, *Stochastic models in operations research: stochastic optimization*, vol. 2, Courier Corporation, 2004.
- [19] M. HUNEULT AND F. D. GALIANA, *A survey of the optimal power flow literature*, IEEE transactions on Power Systems, 6 (1991), pp. 762–770.
- [20] P. KALL AND S. W. WALLACE, *Stochastic programming*, Springer, 1994.
- [21] T. KIM, S. J. WRIGHT, D. BIENSTOCK, AND S. HARNETT, *Analyzing vulnerability of power systems with continuous optimization formulations*, IEEE Transactions on Network Science and Engineering, 3 (2016), pp. 132–146.
- [22] S. H. LOW, *Convex relaxation of optimal power flow—part I: Formulations and equivalence*, IEEE Transactions on Control of Network Systems, 1 (2014), pp. 15–27.
- [23] S. H. LOW, *Convex relaxation of optimal power flow –part II: Exactness*, IEEE Transactions on Control of Network Systems, 1 (2014), pp. 177–189.
- [24] J. MALICK AND H. S. SENDOV, *Clarke generalized Jacobian of the projection onto the cone of positive semidefinite matrices*, Set-Valued Analysis, 14 (2006), pp. 273–293.
- [25] B. L. MILLER AND H. M. WAGNER, *Chance constrained programming with joint constraints*, Operations Research, 13 (1965), pp. 930–945.

- [26] A. MOHAPATRA, P. BIJWE, AND B. PANIGRAHI, *An OPF sensitivity based approach for handling discrete variables*, in PES General Meeting— Conference & Exposition, 2014 IEEE, IEEE, 2014, pp. 1–5.
- [27] D. K. MOLZAHN, I. A. HISKENS, ET AL., *A survey of relaxations and approximations of the power flow equations*, Foundations and Trends® in Electric Energy Systems, 4 (2019), pp. 1–221.
- [28] J. M. MULVEY, R. J. VANDERBEI, AND A. S. ZENIOS, *Robust optimization of large-scale systems*, Operations research, 43 (1995), pp. 264–281.
- [29] B. O’DONOGHUE, E. CHU, N. PARIKH, AND S. BOYD, *Conic optimization via operator splitting and homogeneous self-dual embedding*, Journal of Optimization Theory and Applications, 169 (2016), pp. 1042–1068.
- [30] L. ROALD AND D. K. MOLZAHN, *Implied constraint satisfaction in power system optimization: The impacts of load variations*, arXiv preprint arXiv:1904.01757, (2019).
- [31] R. T. ROCKAFELLAR, *Convex analysis*, Princeton university press, 2015.
- [32] B. STOTT, J. JARDIM, AND O. ALSAÇ, *DC power flow revisited*, IEEE Transactions on Power Systems, 24 (2009), pp. 1290–1300.
- [33] J. SUN AND L. TESFATSION, *DC optimal power flow formulation and solution using QuadProgJ*, Iowa State University Digital Repository, (2010).
- [34] Y. TANG, E. DALL’ANESE, A. BERNSTEIN, AND S. LOW, *Running primal-dual gradient method for time-varying nonconvex problems*, arXiv preprint arXiv:1812.00613, (2018).
- [35] A. J. WOOD AND B. F. WOLLENBERG, *Power generation, operation, and control*, John Wiley & Sons, 2012.
- [36] Y. YE, M. J. TODD, AND S. MIZUNO, *An $O(\sqrt{nl})$ -iteration homogeneous and self-dual linear programming algorithm*, Mathematics of Operations Research, 19 (1994), pp. 53–67.
- [37] C. YU, *Sensitivity analysis of multi-area optimum power flow solutions*, Electric Power Systems Research, 58 (2001), pp. 149–155.
- [38] X.-S. ZHANG AND D.-G. LIU, *A note on the continuity of solutions of parametric linear programs*, Mathematical Programming, 47 (1990), pp. 143–153.
- [39] F. ZHOU, J. ANDERSON, AND S. H. LOW, *Differential privacy of aggregated DC optimal power flow data*, Accepted to the 2019 American Control Conference, arXiv preprint arXiv:1903.11237, (2019).

- [40] R. D. ZIMMERMAN, C. E. MURILLO-SÁNCHEZ, AND R. J. THOMAS, *MATPOWER: Steady-state operations, planning, and analysis tools for power systems research and education*, IEEE Transactions on power systems, 26 (2011), pp. 12–19.

A Proof of Proposition 2.1

As it is trivial that $\text{clos}(\text{int}(\Omega_\xi)) \subseteq \text{clos}(\Omega_\xi)$, we only need to show $\text{clos}(\Omega_\xi) \subseteq \text{clos}(\text{int}(\Omega_\xi))$. It is sufficient to show that $\forall \xi \in \Omega_\xi$, there exists a sequence $(\xi_{(n)})_{n=1}^\infty$ such that $\lim_{n \rightarrow \infty} \xi_{(n)} = \xi$ and for each $n \in \mathbb{Z}_+$ there is an open neighborhood $U(\xi_{(n)}) \ni \xi_{(n)}$ such that $U(\xi_{(n)}) \subseteq \Omega_\xi$. The reason is as follows, by definition, any point in $\text{clos}(\Omega_\xi)$ is the limit of a sequence of points in Ω_ξ . If any point in Ω_ξ is further the limit of a sequence of points in $\text{int}(\Omega_\xi)$, then any point in $\text{clos}(\Omega_\xi)$ can also be represented as the limit of a sequence of points in $\text{int}(\Omega_\xi)$. That is to say, $\text{clos}(\Omega_\xi) \subseteq \text{clos}(\text{int}(\Omega_\xi))$. Next we prove $\forall \xi \in \Omega_\xi$, such sequence $(\xi_{(n)})_{n=1}^\infty$ exists.

First, we observe that (3b)-(3e) implies the branch power flow $\mathbf{p} := \mathbf{BC}^\top \boldsymbol{\theta}$ satisfies

$$\mathbf{p} = \mathbf{BC}^\top (\mathbf{CBC}^\top)^\dagger \begin{bmatrix} \mathbf{s}^g \\ -\mathbf{s}^l \end{bmatrix}.$$

We use ρ to denote the matrix norm of $\mathbf{BC}^\top (\mathbf{CBC}^\top)^\dagger$ induced by the ℓ_1 vector norm:

$$\rho := \max_{\mathbf{x} \neq \mathbf{0}} \frac{\|\mathbf{BC}^\top (\mathbf{CBC}^\top)^\dagger \mathbf{x}\|_1}{\|\mathbf{x}\|_1}.$$

Now consider any $\hat{\xi} = [(\bar{\mathbf{s}}^g)^\top, (\underline{\mathbf{s}}^g)^\top, \bar{\mathbf{p}}^\top, \underline{\mathbf{p}}^\top]^\top \in \Omega_\xi$ with $\underline{\mathbf{s}}^g \geq 0$, and there exists $(\hat{\mathbf{s}}^g, \hat{\mathbf{s}}^l)$ such that $\hat{\mathbf{s}}^l > 0$ and (3b)-(3e) are satisfied (with associated branch power flow $\hat{\mathbf{p}}$). Then we construct $\xi_{(n)}$ as

$$\xi_{(n)} = \begin{bmatrix} \bar{\mathbf{s}}^g + \frac{3}{n} \mathbf{1}_{N_G} \\ \underline{\mathbf{s}}^g + \frac{1}{n} \mathbf{1}_{N_G} \\ \bar{\mathbf{p}} + 5\rho \frac{N_G}{n} \mathbf{1}_E \\ \underline{\mathbf{p}} - 5\rho \frac{N_G}{n} \mathbf{1}_E \end{bmatrix}$$

and its open neighborhood

$$U(\xi_{(n)}) = \left\{ \xi \mid - \begin{bmatrix} \frac{1}{n} \mathbf{1}_{2N_G} \\ \rho \frac{N_G}{n} \mathbf{1}_{2E} \end{bmatrix} < \xi - \xi_{(n)} < \begin{bmatrix} \frac{1}{n} \mathbf{1}_{2N_G} \\ \rho \frac{N_G}{n} \mathbf{1}_{2E} \end{bmatrix} \right\}.$$

Clearly, $\xi_{(n)}$ converges to $\hat{\xi}$ as $n \rightarrow \infty$. Next, we are going to prove that for any $\xi \in U(\xi_{(n)})$, we have $\xi \in \Omega_\xi$. For the convenience of notation, we use $\bar{\mathbf{s}}^g(\xi)$, $\underline{\mathbf{s}}^g(\xi)$, $\bar{\mathbf{p}}(\xi)$, $\underline{\mathbf{p}}(\xi)$ to denote the corresponding part in ξ . Since for any $i \in \mathcal{V}_G$

$$\underline{\mathbf{s}}_i^g(\xi) > \underline{\mathbf{s}}_i^g(\xi_{(n)}) - \frac{1}{n} = \underline{\mathbf{s}}_i^g(\hat{\xi}) + \frac{1}{n} - \frac{1}{n} = \underline{\mathbf{s}}_i^g(\hat{\xi}) \geq 0,$$

we only need to check if there exist $(\mathbf{s}^g, \mathbf{s}^l)$ such that (3b)-(3e) are satisfied and $\mathbf{s}^l > 0$. We construct $\mathbf{s}^g = \hat{\mathbf{s}}^g + \frac{2}{n}\mathbf{1}_{N_G}$ and $\mathbf{s}^l = \hat{\mathbf{s}}^l + \frac{2N_G}{nN_L}\mathbf{1}_{N_L}$, then it is clear that $\mathbf{s}^l \geq \hat{\mathbf{s}}^l > 0$. Since $\mathbf{1}_{N_G}^\top \mathbf{s}^g = \mathbf{1}_{N_G}^\top \hat{\mathbf{s}}^g + \frac{2N_G}{n} = \mathbf{1}_{N_L}^\top \hat{\mathbf{s}}^l + \frac{2N_G}{n} = \mathbf{1}_{N_L}^\top \mathbf{s}^l$, the constructed generation and load are balanced so (3c) is satisfied for some $\boldsymbol{\theta}$. Further, we can always shift $\boldsymbol{\theta}$ to make $\theta_1 = 0$ and (3b) is thereby satisfied. Next, we can check

$$\begin{aligned}\mathbf{s}^g &= \hat{\mathbf{s}}^g + \frac{1}{n}\mathbf{1}_{N_G} + \frac{1}{n}\mathbf{1}_{N_G} \geq \underline{\mathbf{s}}^g(\boldsymbol{\xi}_{(n)}) + \frac{1}{n}\mathbf{1}_{N_G} > \underline{\mathbf{s}}^g(\boldsymbol{\xi}) \\ \mathbf{s}^g &= \hat{\mathbf{s}}^g + \frac{3}{n}\mathbf{1}_{N_G} - \frac{1}{n}\mathbf{1}_{N_G} \leq \bar{\mathbf{s}}^g(\boldsymbol{\xi}_{(n)}) - \frac{1}{n}\mathbf{1}_{N_G} < \bar{\mathbf{s}}^g(\boldsymbol{\xi}),\end{aligned}$$

thus (3d) is satisfied. Finally,

$$\mathbf{p} = \mathbf{B}\mathbf{C}^\top(\mathbf{C}\mathbf{B}\mathbf{C}^\top)^\dagger \begin{bmatrix} \hat{\mathbf{s}}^g + \frac{2}{n}\mathbf{1}_{N_G} \\ -\hat{\mathbf{s}}^l - \frac{2N_G}{nN_L}\mathbf{1}_{N_L} \end{bmatrix} = \hat{\mathbf{p}} + \mathbf{B}\mathbf{C}^\top(\mathbf{C}\mathbf{B}\mathbf{C}^\top)^\dagger \begin{bmatrix} \frac{2}{n}\mathbf{1}_{N_G} \\ -\frac{2N_G}{nN_L}\mathbf{1}_{N_L} \end{bmatrix},$$

so

$$\begin{aligned}\mathbf{p}_i &\geq \hat{\mathbf{p}}_i - \left\| \mathbf{B}\mathbf{C}^\top(\mathbf{C}\mathbf{B}\mathbf{C}^\top)^\dagger \begin{bmatrix} \frac{2}{n}\mathbf{1}_{N_G} \\ -\frac{2N_G}{nN_L}\mathbf{1}_{N_L} \end{bmatrix} \right\|_1 \geq \underline{\mathbf{p}}_i(\hat{\boldsymbol{\xi}}) - \rho \cdot \left(\frac{2}{n}N_G + \frac{2N_G}{nN_L}N_L \right) \\ &= \underline{\mathbf{p}}_i(\hat{\boldsymbol{\xi}}) - 4\rho \frac{N_G}{n} = \underline{\mathbf{p}}_i(\boldsymbol{\xi}_{(n)}) + \rho \frac{N_G}{n} > \underline{\mathbf{p}}_i(\boldsymbol{\xi})\end{aligned}$$

and similarly $\mathbf{p}_i < \bar{\mathbf{p}}_i(\boldsymbol{\xi})$. As the result, we have $\underline{\mathbf{p}}(\boldsymbol{\xi}) \leq \mathbf{p} \leq \bar{\mathbf{p}}(\boldsymbol{\xi})$ and (3e) is satisfied.

Above all, we have shown that there exist $(\mathbf{s}^g, \mathbf{s}^l)$ such that (3b)-(3e) are satisfied and $\mathbf{s}^l > 0$. Thus $\boldsymbol{\xi} \in \Omega_{\boldsymbol{\xi}}$ and there must be $U(\boldsymbol{\xi}_{(n)}) \subseteq \Omega_{\boldsymbol{\xi}}$.

B Proof of Proposition 3.1

We first define

$$\Omega_{\mathbf{f}}^{(1)} = \{\mathbf{f} \in \mathbb{R}_+^{N_G} \mid \forall \boldsymbol{\xi} \in \Omega_{\boldsymbol{\xi}}, \forall \mathbf{s}^l \in \Omega_{\mathbf{s}^l}(\boldsymbol{\xi}), (3) \text{ has unique optimal solution}\} \quad (19a)$$

$$\Omega_{\mathbf{f}}^{(2)} = \{\mathbf{f} \in \mathbb{R}_+^{N_G} \mid \forall \boldsymbol{\xi} \in \Omega_{\boldsymbol{\xi}}, \forall \mathbf{s}^l \in \Omega_{\mathbf{s}^l}(\boldsymbol{\xi}), \text{all solutions of (4) satisfy (5)}\}, \quad (19b)$$

then $\Omega_{\mathbf{f}} = \Omega_{\mathbf{f}}^{(1)} \cap \Omega_{\mathbf{f}}^{(2)}$. For $\mathcal{S} \subseteq \mathcal{E}$, $\mathcal{T} \subseteq \mathcal{V}_G$ such that $|\mathcal{S}| + |\mathcal{T}| \leq N_G - 2$, we construct $\mathcal{Q}(\mathcal{S}, \mathcal{T})$ to be the set of \mathbf{f} such that $\exists \boldsymbol{\tau} \in \mathbb{R}^{N+1}, \boldsymbol{\mu} \in \mathbb{R}^E, \boldsymbol{\lambda} \in \mathbb{R}^{N_G}$ satisfying:

$$\mathbf{0} = \mathbf{M}^\top \boldsymbol{\tau} + \mathbf{C}\mathbf{B}\boldsymbol{\mu} \quad (20a)$$

$$-\mathbf{f} = -[\boldsymbol{\tau}_1, \boldsymbol{\tau}_2, \dots, \boldsymbol{\tau}_{N_G}]^\top + \boldsymbol{\lambda} \quad (20b)$$

$$\boldsymbol{\mu}_i \neq 0 \Rightarrow i \in \mathcal{S} \quad (20c)$$

$$\boldsymbol{\lambda}_i \neq 0 \Rightarrow i \in \mathcal{T}. \quad (20d)$$

When \mathcal{S} and \mathcal{T} are fixed, the vector $\mathbf{C}\mathbf{B}\boldsymbol{\mu}$ takes value in an $|\mathcal{S}|$ dimensional subspace. Since $\text{rank}(\mathbf{M}) = N$, the possible values of $\boldsymbol{\tau}$ must fall within an $|\mathcal{S}| + 1$ dimensional subspace.

Therefore, (20b) implies that \mathbf{f} must be in an $|\mathcal{S}| + 1 + |\mathcal{T}| \leq N_G - 1$ dimensional subspace, and hence $\text{int}(\text{clos}(\mathcal{Q}(\mathcal{S}, \mathcal{T}))) = \emptyset$. Denote

$$\mathcal{Q}_\cup := \left(\bigcup_{\substack{\mathcal{S} \subseteq \mathcal{E}, \mathcal{T} \subseteq \mathcal{V}_G \\ |\mathcal{S}| + |\mathcal{T}| \leq N_G - 2}} \mathcal{Q}(\mathcal{S}, \mathcal{T}) \right),$$

then, $\mathcal{Q}_\cup \cap \mathbb{R}_+^{N_G}$ is nowhere dense in $\mathbb{R}_+^{N_G}$.

On one hand, (19b) and (20) imply that

$$\begin{aligned} \mathbb{R}_+^{N_G} \setminus \Omega_{\mathbf{f}}^{(2)} &= \{\mathbf{f} \in \mathbb{R}_+^{N_G} \mid \exists \boldsymbol{\xi} \in \Omega_{\boldsymbol{\xi}}, \mathbf{s}^l \in \Omega_{\mathbf{s}^l}(\boldsymbol{\xi}), \text{one solution of (4) violates (5)}\} \\ &\subseteq \mathcal{Q}_\cup. \end{aligned}$$

Thereby, $\mathbb{R}_+^{N_G} \setminus \mathcal{Q}_\cup \subseteq \Omega_{\mathbf{f}}^{(2)}$.

On the other hand, we reformulate (3) as

$$\begin{aligned} &\underset{\mathbf{x} := [(\mathbf{s}^g)^\top, \boldsymbol{\theta}^\top]^\top}{\text{minimize}} && [\mathbf{f}^\top, \mathbf{0}^\top] \mathbf{x} \end{aligned} \quad (21a)$$

$$\text{subject to} \quad \mathbf{A}_{\text{eq}} \mathbf{x} = \mathbf{b}_{\text{eq}} \quad (21b)$$

$$\mathbf{A}_{\text{in}} \mathbf{x} \leq \mathbf{b}_{\text{in}} \quad (21c)$$

where

$$\mathbf{A}_{\text{eq}} := \begin{bmatrix} \mathbf{0}^{1 \times N_G} & \mathbf{e}_1 \\ -\mathbf{I}^{N_G} & \mathbf{C} \mathbf{B} \mathbf{C}^\top \\ \mathbf{0}^{N_L \times N_G} & \end{bmatrix}, \quad \mathbf{b}_{\text{eq}} := \begin{bmatrix} \mathbf{0}^{(1+N_G) \times 1} \\ -\mathbf{s}^l \end{bmatrix}, \quad (22a)$$

$$\mathbf{A}_{\text{in}} := \begin{bmatrix} \mathbf{0}^{E \times N_G} & \mathbf{B} \mathbf{C}^\top \\ \mathbf{0}^{E \times N_G} & -\mathbf{B} \mathbf{C}^\top \\ \mathbf{I}^{N_G} & \mathbf{0}^{N_G \times N} \\ -\mathbf{I}^{N_G} & \mathbf{0}^{N_G \times N} \end{bmatrix}, \quad \mathbf{b}_{\text{in}} := \begin{bmatrix} \bar{\mathbf{p}} \\ -\mathbf{p} \\ \bar{\mathbf{s}}^g \\ -\underline{\mathbf{s}}^g \end{bmatrix}. \quad (22b)$$

Geometrically, an LP has multiple optimal solutions if and only if the objective vector is normal to the hyperplane defined by equality constraints and the set of inequality constraints which are binding for all the optimal solutions (i.e., corresponding rows in \mathbf{A}_{eq} and \mathbf{A}_{in}). We collect the rows in \mathbf{A}_{in} which correspond to binding inequality constraints (for all the optimal solutions) and form a new matrix $\tilde{\mathbf{A}}_{\text{in}}$. Formally, let \mathcal{X} be the set of indices i such that the i^{th} row of \mathbf{A}_{in} corresponds to a binding constraint for all the optimal solutions, then $\tilde{\mathbf{A}}_{\text{in}} = \mathbf{I}_{\mathcal{X}} \mathbf{A}_{\text{in}}$. In our case, the objective vector $[\mathbf{f}^\top, \mathbf{0}^\top]^\top$ is an $N_G + N$ dimensional vector, thus the row space of $[\mathbf{A}_{\text{eq}}^\top, \tilde{\mathbf{A}}_{\text{in}}^\top]^\top$ must have dimension $\leq N_G + N - 1$ and $[\mathbf{f}^\top, \mathbf{0}^\top]^\top$ must be within this row space. As \mathbf{A}_{eq} has $N + 1$ linearly independent rows, we can always find $\leq N_G - 2$ independent rows of $\tilde{\mathbf{A}}_{\text{in}}$ to form a new matrix $\tilde{\tilde{\mathbf{A}}}_{\text{in}}$ such that $[\mathbf{A}_{\text{eq}}^\top, \tilde{\tilde{\mathbf{A}}}_{\text{in}}^\top]^\top$ and $[\mathbf{A}_{\text{eq}}^\top, \tilde{\mathbf{A}}_{\text{in}}^\top]^\top$ share the same row space. As a result, $[\mathbf{f}^\top, \mathbf{0}^\top]^\top$ can be represented as the linear combination of rows in $[\mathbf{A}_{\text{eq}}^\top, \tilde{\tilde{\mathbf{A}}}_{\text{in}}^\top]^\top$, and one can always find $(\mathcal{S}, \mathcal{T}, \boldsymbol{\tau}, \boldsymbol{\mu}, \boldsymbol{\lambda})$ satisfying (20) and also $|\mathcal{S}| + |\mathcal{T}| \leq N_G - 2$. Hence $\mathbb{R}_+^{N_G} \setminus \Omega_{\mathbf{f}}^{(1)}$ is also a subset of \mathcal{Q}_\cup and thus $\mathbb{R}_+^{N_G} \setminus \mathcal{Q}_\cup \subseteq \Omega_{\mathbf{f}}^{(1)}$.

Above all, $\mathbb{R}_+^{N_G} \setminus \mathcal{Q}_\cup \subseteq \Omega_{\mathbf{f}}^{(1)} \cap \Omega_{\mathbf{f}}^{(2)} = \Omega_{\mathbf{f}}$. Since $\mathcal{Q}_\cup \cap \mathbb{R}_+^{N_G}$ is nowhere dense in $\mathbb{R}_+^{N_G}$, $\Omega_{\mathbf{f}}$ is dense in $\mathbb{R}_+^{N_G}$.

C Proof of Proposition 3.3

We require the following auxiliary lemma to prove Proposition 3.3.

Lemma C.1. *Suppose the set $\mathcal{S} \subseteq \mathbb{R}^n$ satisfies the condition that $\text{clos}(\text{int}(\mathcal{S})) = \text{clos}(\mathcal{S})$, and \mathcal{T} is an affine hyperplane with dimension strictly less than n . Then \mathcal{T} is nowhere dense in \mathcal{S} .*

Proof. If not, then by definition, in the relative topology of \mathcal{S} , we have $\text{int}(\mathcal{T}) \neq \emptyset$ since \mathcal{T} is closed. Pick any point $\mathbf{x} \in \text{int}(\mathcal{T})$, there must be an n -dimensional open ball U with radius r centered at \mathbf{x} such that $\mathbf{x} \in U \cap \mathcal{S} \subseteq \mathcal{T}$. In the n -dimensional Euclidean topology, since $\text{clos}(\text{int}(\mathcal{S})) = \text{clos}(\mathcal{S})$, there must be a point $\mathbf{x}_1 \in \mathcal{S}$ such that $|\mathbf{x} - \mathbf{x}_1| \leq r/2$ and there is an n -dimensional open ball U_1 centered at \mathbf{x}_1 and have radius $< r/2$ satisfying $U_1 \subseteq \mathcal{S}$. Clearly, $U_1 \subseteq U$ as well, and thereby $U_1 \subseteq U \cap \mathcal{S} \subseteq \mathcal{T}$. However, \mathcal{T} is an affine hyperplane with dimension strictly less than n , and there is the contradiction. ■

We are now in a position to prove Proposition 3.3. Our strategy is to construct the set $\tilde{\Omega}_\xi(\mathbf{f})$ first, and then prove $\text{clos}(\text{int}(\Omega_{\mathbf{s}^l}(\xi))) = \text{clos}(\Omega_{\mathbf{s}^l}(\xi))$ and $\tilde{\Omega}_{\mathbf{s}^l}(\xi, \mathbf{f})$ is dense in $\Omega_{\mathbf{s}^l}(\xi)$ respectively.

Consider the power flow equations below:

$$\mathbf{T}\boldsymbol{\theta} := \begin{bmatrix} \mathbf{C}\mathbf{B}\mathbf{C}^\top \\ \mathbf{B}\mathbf{C}^\top \end{bmatrix} \boldsymbol{\theta} = \begin{bmatrix} \mathbf{s}^g \\ -\mathbf{s}^l \\ \mathbf{p} \end{bmatrix}. \quad (23)$$

Proposition 3.1 and Assumption 2 show that there will always be at least $N_G - 1$ binding inequality constraints as each non-zero multiplier will force one inequality constraint to be binding. A constraint being binding means some \mathbf{s}_i^g equals either $\bar{\mathbf{s}}_i^g$ or $\underline{\mathbf{s}}_i^g$ (as in the upper N_G rows in (23)), or some \mathbf{p}_i equals either $\bar{\mathbf{p}}_i$ or $\underline{\mathbf{p}}_i$ (as in the lower E rows in (23)). We have $\text{rank}(\mathbf{T}) = N - 1$. We use the following procedure to construct the set $\tilde{\Omega}_\xi$.

$$\text{I. } \tilde{\Omega}_\xi \leftarrow \Omega_\xi \setminus \left(\left(\bigcup_{i \in \mathcal{V}_G} \{\xi \mid \xi_i = \xi_{i+N_G}\} \right) \cup \left(\bigcup_{i=2N_G \in \mathcal{E}} \{\xi \mid \xi_i = \xi_{i+E}\} \right) \right)$$

II. For each $\mathcal{S} \subseteq \mathcal{V}_G \cup [N+1, N+E]$, construct $\mathbf{T}_\mathcal{S}$.

- a) If $\text{rank}(\mathbf{T}_\mathcal{S}) = |\mathcal{S}|$, then continue to another \mathcal{S} .
- b) If $\text{rank}(\mathbf{T}_\mathcal{S}) < |\mathcal{S}|$, then consider

$$\Gamma := \prod_{i \in \mathcal{S} \cap \mathcal{V}_G} \{\mathbf{e}_i, \mathbf{e}_{N_G+i}\} \times \prod_{\substack{j \in \mathcal{E} \\ j+N \in \mathcal{S}}} \{\mathbf{e}_{2N_G+j}, \mathbf{e}_{2N_G+E+j}\}. \quad (24)$$

Now update $\tilde{\Omega}_\xi$ as

$$\tilde{\Omega}_\xi \leftarrow \tilde{\Omega}_\xi \setminus \bigcup_{\gamma \in \Gamma} \{\xi \mid \exists \boldsymbol{\theta}, \text{ such that } \gamma^\top \xi = \mathbf{T}_\mathcal{S} \boldsymbol{\theta}\}. \quad (25)$$

III. Return $\tilde{\Omega}_\xi$.

In the above procedure, an n -tuple of vectors is also regarded as a matrix of n columns and the product in Eq. (24) is Cartesian product.⁵ Since $\gamma \in \Gamma$ is of rank $|\mathcal{S}|$ and $\mathbf{T}_\mathcal{S}\boldsymbol{\theta}$ with $\boldsymbol{\theta} \in \mathbb{R}^N$ defines a subspace of $\leq |\mathcal{S}| - 1$ dimensions, each set of $\{\boldsymbol{\xi} \mid \exists \boldsymbol{\theta}, \text{ such that } \gamma^\top \boldsymbol{\xi} = \mathbf{T}_\mathcal{S}\boldsymbol{\theta}\}$ in (25) is a subspace with dimension strictly lower than $2N_G + 2E$, and is thereby nowhere dense in Ω_ξ by Lemma C.1. Similarly, the sets $\{\boldsymbol{\xi} \mid \boldsymbol{\xi}_i = \boldsymbol{\xi}_{i+N_G}\}$ for $i \in \mathcal{V}_G$ and $\{\boldsymbol{\xi} \mid \boldsymbol{\xi}_i = \boldsymbol{\xi}_{i+E}\}$ for $i - 2N_G \in \mathcal{E}$ are also nowhere dense. As a result, we have that $\tilde{\Omega}_\xi$ is dense in Ω_ξ . It is sufficient to show that two conditions in Proposition 3.3 are satisfied.

To show $\text{clos}(\text{int}(\Omega_{\mathbf{s}^l}(\boldsymbol{\xi}))) = \text{clos}(\Omega_{\mathbf{s}^l}(\boldsymbol{\xi}))$, it is sufficient to prove that fix $\boldsymbol{\xi} \in \tilde{\Omega}_\xi$, $\forall \hat{\mathbf{s}}^l \in \Omega_{\mathbf{s}^l}(\boldsymbol{\xi})$, there exists a sequence $(\mathbf{s}_{(n)}^l)_{n=1}^\infty$ such that $\lim_{n \rightarrow \infty} \mathbf{s}_{(n)}^l = \hat{\mathbf{s}}^l$ and each $\mathbf{s}_{(n)}^l$ has an open neighborhood $U(\mathbf{s}_{(n)}^l)$ such that $U(\mathbf{s}_{(n)}^l) \subseteq \Omega_{\mathbf{s}^l}(\boldsymbol{\xi})$. By definition, there exists $\hat{\mathbf{s}}^g$ and $\hat{\boldsymbol{\theta}}$ such that (3b)-(3e) are satisfied for $\hat{\mathbf{s}}^l$. We also use $\hat{\mathbf{p}}$ to denote the branch power flow associated with $(\hat{\mathbf{s}}^g, \hat{\mathbf{s}}^l)$. Here we overload $\mathcal{S} \subseteq \mathcal{V}_G \cup [N+1, N+E]$ to denote the indices of all the binding inequality constraints for $(\hat{\mathbf{s}}^g, \hat{\mathbf{s}}^l)$.⁶ By construction, we have $\text{rank}(\mathbf{T}_\mathcal{S}) = |\mathcal{S}| \leq \text{rank}(\mathbf{T}) = N - 1$. There are two situations to discuss: $|\mathcal{S}| = 0$ and $1 \leq |\mathcal{S}| \leq N - 1$.

In the first case, if $|\mathcal{S}| = 0$, then let ρ_1 be the matrix norm of

$$\mathbf{T}_{\mathcal{V}_G \cup [N+1, N+E]} \begin{bmatrix} \mathbf{e}_1^\top \\ \mathbf{T}_{\mathcal{V}_L} \end{bmatrix}^\dagger$$

induced by the ℓ_1 vector norm. Let

$$\epsilon_1 = \min \left\{ \min_{\substack{i \in \mathcal{V}_G \\ \hat{\mathbf{s}}_i^g > \underline{\mathbf{s}}_i^g}} \hat{\mathbf{s}}_i^g - \underline{\mathbf{s}}_i^g, \min_{\substack{i \in \mathcal{V}_G \\ \hat{\mathbf{s}}_i^g > \underline{\mathbf{s}}_i^g}} \bar{\mathbf{s}}_i^g - \hat{\mathbf{s}}_i^g, \min_{\substack{i \in \mathcal{E} \\ \hat{\mathbf{p}}_i > \underline{\mathbf{p}}_i}} \hat{\mathbf{p}}_i - \underline{\mathbf{p}}_i, \min_{\substack{i \in \mathcal{E} \\ \hat{\mathbf{p}}_i > \underline{\mathbf{p}}_i}} \bar{\mathbf{p}}_i - \hat{\mathbf{p}}_i \right\} \quad (26)$$

$$\epsilon_2 = \min_i \hat{\mathbf{s}}_i^l. \quad (27)$$

Here, we have used min. as short hand for minimize. Now we can construct $\mathbf{s}_{(n)}^l \equiv \hat{\mathbf{s}}^l$, and

$$U(\mathbf{s}_{(n)}^l) = \left\{ \mathbf{s}^l \mid |\mathbf{s}^l - \mathbf{s}_{(n)}^l| < \frac{1}{2} \min \left\{ \frac{\epsilon_1}{N_L \rho_1}, \epsilon_2 \right\} \mathbf{1}_{N_L} \right\}.$$

⁵Hence, each $\gamma \in \Gamma$ can also be regarded as a $(2N_G + 2E)$ -by- $|\mathcal{S}|$ matrix. For instance, if we have $\mathcal{S} = \{1, 4, N+2\}$, then

$$\begin{aligned} \Gamma &= \{\mathbf{e}_1, \mathbf{e}_{N_G+1}\} \times \{\mathbf{e}_4, \mathbf{e}_{N_G+4}\} \times \{\mathbf{e}_{2N_G+2}, \mathbf{e}_{2N_G+E+2}\} \\ &= \{(\mathbf{e}_1, \mathbf{e}_4, \mathbf{e}_{2N_G+2}), (\mathbf{e}_1, \mathbf{e}_4, \mathbf{e}_{2N_G+E+2}), (\mathbf{e}_1, \mathbf{e}_{N_G+4}, \mathbf{e}_{2N_G+2}), (\mathbf{e}_1, \mathbf{e}_{N_G+4}, \mathbf{e}_{2N_G+E+2}), \\ &\quad (\mathbf{e}_{N_G+1}, \mathbf{e}_4, \mathbf{e}_{2N_G+2}), (\mathbf{e}_{N_G+1}, \mathbf{e}_4, \mathbf{e}_{2N_G+E+2}), (\mathbf{e}_{N_G+1}, \mathbf{e}_{N_G+4}, \mathbf{e}_{2N_G+2}), (\mathbf{e}_{N_G+1}, \mathbf{e}_{N_G+4}, \mathbf{e}_{2N_G+E+2})\} \\ &= \{[\mathbf{e}_1 \ \mathbf{e}_4 \ \mathbf{e}_{2N_G+2}], [\mathbf{e}_1 \ \mathbf{e}_4 \ \mathbf{e}_{2N_G+E+2}], [\mathbf{e}_1 \ \mathbf{e}_{N_G+4} \ \mathbf{e}_{2N_G+2}], [\mathbf{e}_1 \ \mathbf{e}_{N_G+4} \ \mathbf{e}_{2N_G+E+2}], \\ &\quad [\mathbf{e}_{N_G+1} \ \mathbf{e}_4 \ \mathbf{e}_{2N_G+2}], [\mathbf{e}_{N_G+1} \ \mathbf{e}_4 \ \mathbf{e}_{2N_G+E+2}], [\mathbf{e}_{N_G+1} \ \mathbf{e}_{N_G+4} \ \mathbf{e}_{2N_G+2}], [\mathbf{e}_{N_G+1} \ \mathbf{e}_{N_G+4} \ \mathbf{e}_{2N_G+E+2}]\} \end{aligned}$$

is a set of 8 elements and each element is a $(2N_G + 2E)$ -by-3 matrix.

⁶In this section, the index of a constraint associated with generator i (either the upper or lower bounds) is i and the index of a constraint associated with branch i (either the upper or lower bounds) is $i + N$. Step I in the procedure constructing $\tilde{\Omega}_\xi$ guarantees that a generator or branch cannot reach the upper and lower bound at the same time.

It is trivial that $\lim_{n \rightarrow \infty} \mathbf{s}_{(n)}^l = \hat{\mathbf{s}}^l$. For any $\mathbf{s}^l \in U(\mathbf{s}_{(n)}^l)$, we have

$$\mathbf{s}^l > \mathbf{s}_{(n)}^l - \frac{1}{2}\epsilon_2 \mathbf{1}_{N_L} = \hat{\mathbf{s}}^l - \left(\frac{1}{2} \min_i \hat{\mathbf{s}}_i^l\right) \mathbf{1}_{N_L} > 0.$$

Further, we will show that for

$$\boldsymbol{\theta} = \begin{bmatrix} \mathbf{e}_1^\top \\ \mathbf{T}_{\mathcal{V}_L} \end{bmatrix}^\dagger \begin{bmatrix} 0 \\ -\mathbf{s}^l \end{bmatrix}, \mathbf{s}^g = \mathbf{T}_{\mathcal{V}_G} \boldsymbol{\theta}, \quad (28)$$

(3b)-(3e) are satisfied. Clearly (28) implies $\mathbf{e}_1^\top \boldsymbol{\theta} = 0$, $\mathbf{T}_{\mathcal{V}_L} \boldsymbol{\theta} = -\mathbf{s}^l$ and $\mathbf{T}_{\mathcal{V}_G} \boldsymbol{\theta} = \mathbf{s}^g$, which are equivalent to (3b), (3c). For (3d), as no $\hat{\mathbf{s}}_i^g$ reaches any bound, we have

$$|\mathbf{s}_i^g - \hat{\mathbf{s}}_i^g| \leq \rho_1 \|\mathbf{s}^l - \hat{\mathbf{s}}^l\|_1 \leq \rho_1 \cdot \frac{1}{2} N_L \frac{\epsilon_1}{N_L \rho_1} = \frac{1}{2} \epsilon_1,$$

and thereby \mathbf{s}_i^g is still strictly between the bounds and stays feasible. Similarly, the branch flow \mathbf{p} is also within the upper and lower bounds, and (3e) is also satisfied. As a result, $\mathbf{s}^l \in \Omega_{\mathbf{s}^l}(\boldsymbol{\xi})$ and thus $U(\hat{\mathbf{s}}^l) \subseteq \Omega_{\mathbf{s}^l}(\boldsymbol{\xi})$.

In the second case, we have $1 \leq |\mathcal{S}| \leq N - 1$, then define

$$\mathbf{T}'(\mathcal{R}) := \begin{bmatrix} \mathbf{e}_1^\top \\ \mathbf{T}_{\mathcal{S}} \\ \mathbf{T}_{\mathcal{R}} \end{bmatrix}, \text{ for } \mathcal{R} \subseteq \mathcal{V}_L.$$

Let $\mathcal{R}^* = \arg \min_{\mathcal{R}: \text{rank}(\mathbf{T}'(\mathcal{R})) = \text{rank}(\mathbf{T}'(\mathcal{V}_L))} |\mathcal{R}|$. If there are multiple \mathcal{R} that minimize $|\mathcal{R}|$ then pick any one of them. There are two simple observations:

- All rows of matrix $\mathbf{T}'(\mathcal{R}^*)$ are independent.
- All rows of $\mathbf{T}_{\mathcal{V}_L}$ are in the row space of $\mathbf{T}'(\mathcal{R}^*)$.

We further define

$$\mathbf{T}''(\mathcal{T}) := \begin{bmatrix} \mathbf{T}'(\mathcal{R}^*) \\ \mathbf{T}_{\mathcal{T}} \end{bmatrix},$$

for $\mathcal{T} \subseteq (\mathcal{V}_G \cap [N+1, N+E]) \setminus \mathcal{S}$. Let

$$\mathcal{T}^* = \arg \min_{\mathcal{T}: \text{rank}(\mathbf{T}''(\mathcal{T})) = \text{rank}(\mathbf{T}''((\mathcal{V}_G \cap [N+1, N+E]) \setminus \mathcal{S}))} |\mathcal{T}|.$$

Likewise, if there are multiple such \mathcal{T} to minimize $|\mathcal{T}|$ then pick any one of them. There are also two simple observations:

- All rows of the matrix $\mathbf{T}''(\mathcal{T}^*)$ are still independent.

- Now all rows of \mathbf{T} are in the row space of $\mathbf{T}''(\mathcal{T}^*)$.

Let ρ_2 be the matrix norm of $\mathbf{T}(\mathbf{T}''(\mathcal{T}^*))^\dagger$ induced by the ℓ_1 vector norm. Let ϵ_1 and ϵ_2 be the same as in (26) and (27), and we define the direction vector $\mathbf{v} \in \mathbb{R}^{|\mathcal{S}|}$ as

$$\mathbf{v} := \text{sgn} \left(\mathbf{T}_S \hat{\boldsymbol{\theta}} - \begin{bmatrix} (\bar{\mathbf{s}}^g)_{S \cap \mathcal{V}_G} \\ (\bar{\mathbf{p}})_{(S-N) \cap \mathcal{E}} \end{bmatrix} \right) + \text{sgn} \left(\mathbf{T}_S \hat{\boldsymbol{\theta}} - \begin{bmatrix} (\underline{\mathbf{s}}^g)_{S \cap \mathcal{V}_G} \\ (\underline{\mathbf{p}})_{(S-N) \cap \mathcal{E}} \end{bmatrix} \right)$$

where sgn applies the sign function to each coordinate of the vector. We then construct

$$\mathbf{s}_{(n)}^l := \mathbf{T}_{\mathcal{V}_L} (\mathbf{T}''(\mathcal{T}^*))^\dagger \begin{bmatrix} 0 \\ \mathbf{T}_S \hat{\boldsymbol{\theta}} - \frac{\min\{\epsilon_1, \epsilon_2\}}{2nN\rho_2} \mathbf{v} \\ \mathbf{T}_{\mathcal{R}^*} \hat{\boldsymbol{\theta}} \\ \mathbf{T}_{\mathcal{T}^*} \hat{\boldsymbol{\theta}} \end{bmatrix}.$$

Since all rows of \mathbf{T} are in the row space of $\mathbf{T}''(\mathcal{T}^*)$, we have

$$(\mathbf{T}''(\mathcal{T}^*))^\dagger \begin{bmatrix} 0 \\ \mathbf{T}_S \hat{\boldsymbol{\theta}} \\ \mathbf{T}_{\mathcal{R}^*} \hat{\boldsymbol{\theta}} \\ \mathbf{T}_{\mathcal{T}^*} \hat{\boldsymbol{\theta}} \end{bmatrix} - \hat{\boldsymbol{\theta}}$$

is perpendicular to the row space of $\mathbf{T}_{\mathcal{V}_L}$. Therefore,

$$\lim_{n \rightarrow \infty} \mathbf{s}_{(n)}^l \rightarrow \mathbf{T}_{\mathcal{V}_L} (\mathbf{T}''(\mathcal{T}^*))^\dagger \begin{bmatrix} 0 \\ \mathbf{T}_S \hat{\boldsymbol{\theta}} \\ \mathbf{T}_{\mathcal{R}^*} \hat{\boldsymbol{\theta}} \\ \mathbf{T}_{\mathcal{T}^*} \hat{\boldsymbol{\theta}} \end{bmatrix} = \mathbf{T}_{\mathcal{V}_L} \hat{\boldsymbol{\theta}} = \hat{\mathbf{s}}^l.$$

Besides, since

$$\hat{\mathbf{s}}^l - \mathbf{s}_{(n)}^l = \mathbf{T}_{\mathcal{V}_L} (\mathbf{T}''(\mathcal{T}^*))^\dagger \begin{bmatrix} 0 \\ \frac{\min\{\epsilon_1, \epsilon_2\}}{2nN\rho_2} \mathbf{v} \\ \mathbf{0}_{(|\mathcal{R}^*| + |\mathcal{T}^*|) \times 1} \end{bmatrix},$$

we have

$$\mathbf{s}_{(n)}^l \geq \hat{\mathbf{s}}^l - \rho_2 |\mathcal{S}| \frac{\epsilon_2}{2nN\rho_2} \mathbf{1}_{N_L} \geq \hat{\mathbf{s}}^l - \frac{\epsilon_2}{2n} \mathbf{1}_{N_L} > 0.$$

We then construct the associated $\boldsymbol{\theta}_{(n)}$, $\mathbf{s}_{(n)}^g$ and $\mathbf{p}_{(n)}$ as

$$\begin{aligned} \boldsymbol{\theta}_{(n)} &:= (\mathbf{T}''(\mathcal{T}^*))^\dagger \begin{bmatrix} 0 \\ \mathbf{T}_S \hat{\boldsymbol{\theta}} - \frac{\min\{\epsilon_1, \epsilon_2\}}{2nN\rho_2} \mathbf{v} \\ \mathbf{T}_{\mathcal{R}^*} \hat{\boldsymbol{\theta}} \\ \mathbf{T}_{\mathcal{T}^*} \hat{\boldsymbol{\theta}} \end{bmatrix}, \\ \mathbf{s}_{(n)}^g &:= \mathbf{T}_{\mathcal{V}_G} \boldsymbol{\theta}_{(n)}, \\ \mathbf{p}_{(n)} &:= \mathbf{T}_{[N+1, N+E]} \boldsymbol{\theta}_{(n)}. \end{aligned}$$

For $\mathbf{s}_{(n)}^g$, we have

$$|\hat{\mathbf{s}}^g - \mathbf{s}_{(n)}^g| = \left| \mathbf{T}_{\mathcal{V}_G} (\mathbf{T}''(\mathcal{T}^*))^\dagger \begin{bmatrix} 0 \\ \frac{\min\{\epsilon_1, \epsilon_2\}}{2nN\rho_2} \mathbf{v} \\ \mathbf{0}_{(|\mathcal{R}^*|+|\mathcal{T}^*|)\times 1} \end{bmatrix} \right| \leq \rho_2 |\mathcal{S}| \frac{\epsilon_1}{2nN\rho_2} \mathbf{1}_{N_G} \leq \frac{\epsilon_1}{2n} \mathbf{1}_{N_G},$$

and consider that all the generators that reach the upper or lower bounds in $\hat{\mathbf{s}}^g$ have been moved towards the opposite directions encoded in \mathbf{v} . All the coordinates in $\mathbf{s}_{(n)}^g$ will then strictly stay within the limits. The similar argument also applies to $\mathbf{p}_{(n)}$ and implies that all the coordinates in $\mathbf{p}_{(n)}$ also strictly stay within the limits. Thereby, $\mathbf{s}_{(n)}^l \in \Omega_{\mathbf{s}^l}(\boldsymbol{\xi})$ and there is no binding constraint associated with $(\mathbf{s}_{(n)}^g, \mathbf{s}_{(n)}^l)$. We have shown in the first case that when no binding constraints arises, there is always an open neighborhood $U(\mathbf{s}_{(n)}^l) \subseteq \Omega_{\mathbf{s}^l}(\boldsymbol{\xi})$. We now establish the proof of $\text{clos}(\text{int}(\Omega_{\mathbf{s}^l}(\boldsymbol{\xi}))) = \text{clos}(\Omega_{\mathbf{s}^l}(\boldsymbol{\xi}))$.

Next, we will further show $\tilde{\Omega}_{\mathbf{s}^l}(\boldsymbol{\xi})$ is dense in $\Omega_{\mathbf{s}^l}(\boldsymbol{\xi})$. In fact, $\forall \boldsymbol{\xi} \in \tilde{\Omega}_{\boldsymbol{\xi}}$, if for some $\mathbf{s}^l \in \Omega_{\mathbf{s}^l}(\boldsymbol{\xi})$, the optimal solution to (3) has $\geq N_G$ tight inequality constraints, then we use $\mathcal{S} \subseteq [N+E] \setminus \mathcal{V}_L$, $|\mathcal{S}| = N_G$ again to denote the indices of any N_G tight inequality constraints. As those N_G inequality constraints are tight, there must exist $\gamma \in \Gamma$, as defined in (24), such that $\gamma^\top \boldsymbol{\xi} = \mathbf{T}_{\mathcal{S}} \boldsymbol{\theta}^*$ for the optimal $\boldsymbol{\theta}^* \in \mathbb{R}^N$. According to (25), $\text{rank}(\mathbf{T}_{\mathcal{S}})$ must be exactly N_G . We now have

$$\gamma^\top \boldsymbol{\xi} = \mathbf{T}_{\mathcal{S}} \boldsymbol{\theta}^* \quad (29a)$$

$$-\mathbf{s}^l = \mathbf{T}_{\mathcal{V}_L} \boldsymbol{\theta}^*. \quad (29b)$$

For each $\gamma \in \Gamma$, as $\text{rank}(\mathbf{T}_{\mathcal{S}}) = N_G$ but $\text{rank}(\mathbf{T}) = N - 1$, the set $\{\mathbf{s}^l \mid \exists \boldsymbol{\theta}^*, (29) \text{ holds}\}$ is a strict subspace in \mathbb{R}^{N_L} and thereby nowhere dense in $\Omega_{\mathbf{s}^l}$ according to Lemma C.1. As the result, we have

$$\tilde{\Omega}_{\mathbf{s}^l} \supseteq \Omega_{\mathbf{s}^l} \setminus \bigcup_{\substack{|\mathcal{S}|=N_G \\ \mathcal{S} \subseteq [N+E] \setminus \mathcal{V}_L}} \bigcup_{\gamma \in \Gamma} \{\mathbf{s}^l \mid \exists \boldsymbol{\theta}^*, (29) \text{ holds for } \gamma\}$$

must be dense in $\Omega_{\mathbf{s}^l}$.

D Proofs of the Lemmas Related to Theorem 4.3

Proof.(Lemma 4.4) We first set $\underline{\mathbf{s}}_i^g \equiv 0$ and $\bar{\mathbf{s}}_i^g \equiv 2$ for all $i \in \mathcal{V}_G$. Let

$$(\mathbf{s}_*^g)_i = \begin{cases} 0, & i \in \mathcal{S}_G \\ 1, & i \notin \mathcal{S}_G \end{cases} \quad (30)$$

and $\mathbf{s}_*^l = \frac{N_G - |\mathcal{S}_G|}{N_L} \mathbf{1}_{N_L}$. The construction here guarantees that all $(\mathbf{s}_*^g)_i$ for $i \in \mathcal{S}_G$ hit the lower bounds, and other $(\mathbf{s}_*^g)_i$ are strictly within the bounds. Then we let

$$\boldsymbol{\theta}_* = \mathbf{M}^\dagger \begin{bmatrix} \mathbf{s}_*^g \\ -\mathbf{s}_*^l \\ 0 \end{bmatrix}, \quad \mathbf{p}_* = \mathbf{B}\mathbf{C}^\top \boldsymbol{\theta}_*$$

where \mathbf{M} is defined in Section 2.2. Let

$$\begin{aligned}\bar{\mathbf{p}}_i &= \begin{cases} (\mathbf{p}_*)_i, & \text{if } i \in \mathcal{S}_B \text{ and } (\mathbf{p}_*)_i \geq 0 \\ \|\mathbf{p}_*\|_\infty + 1, & \text{otherwise} \end{cases}, \\ \underline{\mathbf{p}}_i &= \begin{cases} (\mathbf{p}_*)_i, & \text{if } i \in \mathcal{S}_B \text{ and } (\mathbf{p}_*)_i < 0 \\ -\|\mathbf{p}_*\|_\infty - 1, & \text{otherwise} \end{cases}.\end{aligned}$$

Setting $\boldsymbol{\xi}_* = [(\bar{\mathbf{s}}^g)^\top, (\underline{\mathbf{s}}^g)^\top, \bar{\mathbf{p}}^\top, \underline{\mathbf{p}}^\top]^\top$, it is easy to check that $(\mathbf{s}_*^g, \boldsymbol{\theta}_*)$ is an extreme point of the convex polytope described by (3b)-(3e) under $(\boldsymbol{\xi}_*, \mathbf{s}_*^l)$ since there are exactly $N + N_G$ equality and binding inequality constraints (corresponding to \mathcal{S}_G and \mathcal{S}_B) in total and they are independent as $\mathcal{S}_G \perp \mathcal{S}_B$. Next, consider the following optimization problem:

$$\underset{\mathbf{x}}{\text{minimize}} \quad \mathbf{f}^\top \mathbf{x} \quad (31a)$$

$$\text{subject to} \quad \underline{\mathbf{s}}^g \leq \mathbf{x} \leq \bar{\mathbf{s}}^g \quad (31b)$$

$$\underline{\mathbf{p}} \leq \mathbf{B}\mathbf{C}^\top(\mathbf{C}\mathbf{B}\mathbf{C}^\top)^\dagger \begin{bmatrix} \mathbf{x} \\ -\mathbf{s}^l \end{bmatrix} \leq \bar{\mathbf{p}}.$$

Here (3) and (31) are equivalent to each other in the sense that there is a bijection between their feasible points shown as below.

$$\begin{aligned}(\mathbf{s}_{\text{fea}}^g, \boldsymbol{\theta}_{\text{fea}}) &\rightarrow \mathbf{x}_{\text{fea}} : \mathbf{x}_{\text{fea}} = \mathbf{s}_{\text{fea}}^g \\ \mathbf{x}_{\text{fea}} &\rightarrow (\mathbf{s}_{\text{fea}}^g, \boldsymbol{\theta}_{\text{fea}}) : \mathbf{s}_{\text{fea}}^g = \mathbf{x}_{\text{fea}}, \quad \boldsymbol{\theta}_{\text{fea}} = \mathbf{M}^\dagger \begin{bmatrix} \mathbf{s}_{\text{fea}}^g \\ -\mathbf{s}_*^l \\ 0 \end{bmatrix}.\end{aligned}$$

Since $\boldsymbol{\theta}$ is always linear in \mathbf{s}^g for fixed \mathbf{s}^l , the value of \mathbf{s}_*^g in (30) is also an extreme point of the feasible domain in (31). Therefore there exists $\mathbf{f}' \in \mathbb{R}^{N_G}$ such that when $\mathbf{f} = \mathbf{f}'$ in (31), the optimal solution is uniquely $\mathbf{x}^* = \mathbf{s}_*^g$. The equivalence between (3) and (31) implies that when $\mathbf{f} = \mathbf{f}'$ in (3), the optimal solution is $(\mathbf{s}_*^g, \boldsymbol{\theta}_*)$ and is unique. Finally, we construct $\mathbf{f}_* = \mathbf{f}' + \|\mathbf{f}'\|_\infty \mathbf{1}$, then the optimal solution remains the same as $(\mathbf{s}_*^g, \boldsymbol{\theta}_*)$ and is still unique due to the fact that $\mathbf{1}^\top \mathbf{s}_*^g \equiv \mathbf{1}^\top \mathbf{s}_*^l$, but we now have $\mathbf{f}_* \geq 0$. ■

Proof.(Lemma 4.5) We start from $(\mathbf{f}_*, \boldsymbol{\xi}_*, \mathbf{s}_*^l)$ provided in Lemma 4.4, and then perturb the parameters in a specific order to derive the desired $(\mathbf{f}_{**}, \boldsymbol{\xi}_{**}, W)$.

First, [38] shows that the optimal solution set $\mathcal{OPF}(\mathbf{s}_*^l)$ to (3) for fixed \mathbf{s}_*^l is both upper hemi-continuous and lower hemi-continuous in \mathbf{f} . Now for the convenience of notation, we use $\mathcal{OPF}^{\mathbf{f}}$ to denote $\mathcal{OPF}(\mathbf{s}_*^l)$ under the cost vector vector \mathbf{f} . For now, $\boldsymbol{\xi}$ is chosen to be $\boldsymbol{\xi}_*$. Therefore the optimal solution is $(\mathbf{s}_*^g, \boldsymbol{\theta}_*)$ and $\mathcal{OPF}^{\mathbf{f}_*} = \{\mathbf{s}_*^g\}$. As upper hemi-continuity implies that for any neighborhood U of \mathbf{s}_*^g , there is a neighborhood V of \mathbf{f}_* such that $\forall \mathbf{f} \in V$, $\mathcal{OPF}^{\mathbf{f}} \subseteq U$. Consider that (3) is a linear programming problem, so the optimal solution set should contain at least a different extreme point $((\mathbf{s}^g)', \boldsymbol{\theta}') \neq (\mathbf{s}_*^g, \boldsymbol{\theta}_*)$ if $\mathcal{OPF}^{\mathbf{f}} \neq \{\mathbf{s}_*^g\}$. Here, $(\mathbf{s}^g)' \neq \mathbf{s}_*^g$ must hold as $(\mathbf{s}^g)' = \mathbf{s}_*^g$ implies $\boldsymbol{\theta}' = \boldsymbol{\theta}_*$. Since a compact convex polytope has only finite extreme points, we can always choose U to be small enough that $(\mathbf{s}_*^g, \boldsymbol{\theta}_*)$ is the only extreme point satisfying $\mathbf{s}_*^g \in U$. Then there must be a neighborhood V of \mathbf{f}_* such

that $\forall \mathbf{f} \in V$, $\mathcal{OPF}^{\mathbf{f}} \equiv \{\mathbf{s}_*^g\}$. Proposition 3.1 shows that $\Omega_{\mathbf{f}}$ is dense in $\mathbb{R}_+^{N_G}$, so there must be some $\mathbf{f}_{**} \in U \cap \Omega_{\mathbf{f}}$ and under \mathbf{f}_{**} , $\mathcal{OPF}^{\mathbf{f}_{**}} = \{\mathbf{s}_*^g\}$ and thereby all the binding constraints are the same as the binding constraints under \mathbf{f}_* , which exactly correspond to \mathcal{S}_G and \mathcal{S}_B . In the proof thus far we have taken the parameters in (3) from $(\mathbf{f}_*, \boldsymbol{\xi}_*, \mathbf{s}_*^l)$ to $(\mathbf{f}_{**}, \boldsymbol{\xi}_*, \mathbf{s}_*^l)$.

Next, we are going to perturb $\boldsymbol{\xi}_*$ to some point in $\tilde{\Omega}_{\boldsymbol{\xi}}(\mathbf{f}_{**})$. We know that

- $(\mathbf{s}_*^g, \boldsymbol{\theta}_*)$ is the unique solution to (3).
- All the constraints and the cost function in (3) are linear and thereby twice continuously differentiable in $(\mathbf{s}^g, \boldsymbol{\theta})$ and differentiable in $\boldsymbol{\xi}$.
- Since all the binding constraints exactly correspond to \mathcal{S}_G and \mathcal{S}_B where $\mathcal{S}_G \perp \mathcal{S}_B$, the gradients for all the binding inequalities and equality constraints are independent.
- We have $|\mathcal{S}_G| + |\mathcal{S}_B| = N_G - 1$ binding inequality constraints. Together with the fact that $\mathbf{f}_{**} \in \Omega_{\mathbf{f}}$ and thus (5) holds, strict complementary slackness must hold.

Lemma 4.1 shows the set of binding constraints do not change in a small neighborhood U of $\boldsymbol{\xi}_*$. Proposition 3.3 shows $\tilde{\Omega}_{\boldsymbol{\xi}}(\mathbf{f}_{**})$ is dense in $\Omega_{\boldsymbol{\xi}}$, so there must be some $\boldsymbol{\xi}_{**} \in U \cap \tilde{\Omega}_{\boldsymbol{\xi}}(\mathbf{f}_{**})$ and under $\boldsymbol{\xi}_{**}$, all the binding constraints are the same as the binding constraints under $\boldsymbol{\xi}_*$, which exactly correspond to \mathcal{S}_G and \mathcal{S}_B . At this point, the parameters in (3) have been updated to $(\mathbf{f}_{**}, \boldsymbol{\xi}_{**}, \mathbf{s}_*^l)$.

Finally, using the technique similar to the perturbation around $\boldsymbol{\xi}_*$ above, the set of binding constraints do not change as well when \mathbf{s}^l falls within a small neighborhood U of \mathbf{s}_*^l , so it is sufficient to show $U \cap \tilde{\Omega}_{\mathbf{s}^l}(\boldsymbol{\xi}_{**}, \mathbf{f}_{**})$ contains an open ball W . First, it is easy to find an open ball W' in $U \cap \Omega_{\mathbf{s}^l}(\boldsymbol{\xi}_{**})$ since $\text{clos}(\text{int}(\Omega_{\mathbf{s}^l}(\boldsymbol{\xi}_{**}))) = \text{clos}(\Omega_{\mathbf{s}^l}(\boldsymbol{\xi}_{**}))$ by Proposition 3.3 implies that \mathbf{s}_*^l must be the limit of a sequence of points which are all interior points of $\Omega_{\mathbf{s}^l}(\boldsymbol{\xi}_{**})$. Thus we can always find an interior point of $\Omega_{\mathbf{s}^l}(\boldsymbol{\xi}_{**})$ that is strictly within U and take its neighborhood $W' \subseteq U \cap \Omega_{\mathbf{s}^l}(\boldsymbol{\xi}_{**})$. Next, as $\Omega_{\mathbf{s}^l}(\boldsymbol{\xi}_{**}) \setminus \tilde{\Omega}_{\mathbf{s}^l}(\boldsymbol{\xi}_{**}, \mathbf{f}_{**})$ can be covered by the union of finitely many affine hyperplanes, $W' \setminus (\Omega_{\mathbf{s}^l}(\boldsymbol{\xi}_{**}) \setminus \tilde{\Omega}_{\mathbf{s}^l}(\boldsymbol{\xi}_{**}, \mathbf{f}_{**}))$ must contain a smaller open ball W , which is a subset of $U \cap \tilde{\Omega}_{\mathbf{s}^l}(\boldsymbol{\xi}_{**}, \mathbf{f}_{**})$. ■